UNIVERSITAT ROVIRA i VIRGILI

Impact of Grape Seed (Poly)Phenol Extract on Oxidative Stress and Mitochondrial Dynamics in a Chronic Chronodisrupted Model

Eduardo Gallardo Baena

BACHELOR'S THESIS IN BIOTECHNOLOGY

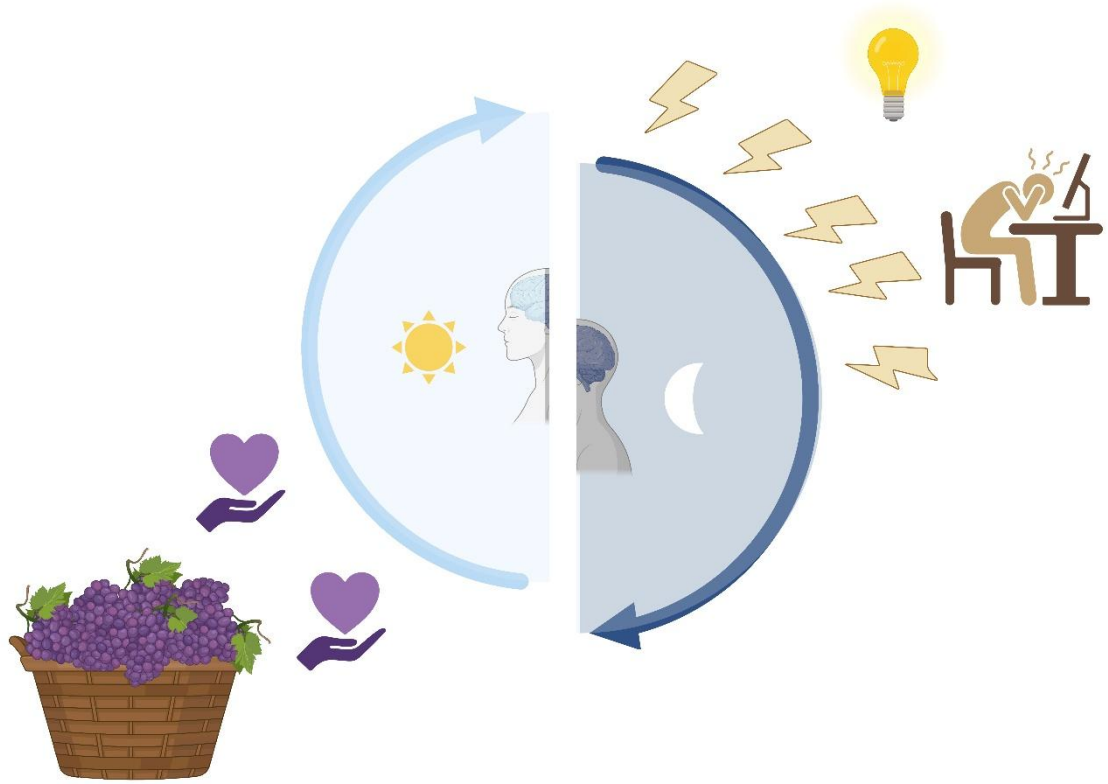

Academic tutor: Dr. Antonio Jesús Cortés Espinar, Departament de Bioquímica i Biotecnologia, antoniojesus.cortes@urv.cat

In coperation with: Nutrigenomics Research group (URV)

Supervisor: Dr. Antonio Jesús Cortés Espinar, Departament de Bioquímica i Biotecnologia, antoniojesus.cortes@urv.cat

Jo, Eduardo Gallardo Baena, amb DNI 48023389X, sóc coneixedor de la guia de prevenció del plagi a la URV *Prevenció, detecció i tractament del plagi en la docència: guia per a estudiants* (aprovada el juliol 2017) (http://www.urv.cat/ca/vidacampus/serveis/crai/que-us-oferim/formacio-competencies-nuclears/plagi/) i afirmo que aquet TFG no constitueixen cap de les conductes considerades com a plagi per la URV.

Tarragona, 3 de septembre de 2025

(signatura)

Table of Contents

Abstract and keywords

Circadian rhythms coordinate key physiological processes such as mitochondrial function and antioxidant defense. Their disruption (chronodisruption), caused by alterations in the light–dark cycle or feeding behavior, has been associated with oxidative stress and metabolic imbalance. Phenolic compounds, including grape seed (poly)phenol extract (GSPE), have shown modulatory effects on redox homeostasis under chronodisruptive conditions. However, the impact of GSPE on chronic circadian disruption induced by a shortened light–dark cycle remains largely unexplored. Therefore, this study evaluated the effects of chronic circadian disruption and GSPE supplementation using male Wistar rats fed a standard diet. Animals were maintained under either a regular 12 h light/12 h dark cycle (L12; 24 h cycle) or a shortened 11 h light/11 h dark cycle (L11; 22 h cycle) and treated daily with GSPE or vehicle for five weeks. After adaptation, rats were euthanized at four time points (ZT3, ZT9, ZT15, ZT21), and liver and plasma samples were collected for gene expression and rhythmicity analyses. The transcriptional profiles of core clock, mitochondrial dynamics, and antioxidant genes were quantified, and diurnal rhythmicity and correlations were evaluated to reveal functional patterns. Interestingly, the GSPE supplementation promoted modulatory effects on hepatic gene expression, counteracting part of the alterations induced by the chronic disruption of the light–dark cycle, which exerted a stronger impact overall. Moreover, diurnal rhythmicity was evident in clock genes but less clear in mitochondrial and antioxidant genes. In conclusion, GSPE displayed partial but consistent modulatory effects under chronic circadian disruption, supporting the notion that (poly)phenols may contribute to mitigating the impact of altered photoperiods. Further studies are warranted to delineate their precise role.

Keywords: Phenolic compounds, diurnal rhythms, circadian rhythms, liver, chronodisruption, oxidative stress, mitochondrial dynamics, GSPE.

Introduction

Biological rhythms

Organisms are constantly exposed to environmental fluctuations, such as changes in temperature and light/dark cycles, which can critically affect survival. To optimize energy efficiency and enhance biological fitness, they have evolved mechanisms that anticipate and adapt to these changes through physiological adjustments, thereby conferring an evolutionary advantage. This adaptive capacity underlies the emergence of biological rhythms, endogenous patterns that regulate behavior, metabolism, and other physiological processes in response to environmental cues (Lee et al., 2021).

Among the most predictable of these fluctuations are those driven by the Earth's rotation and revolution, which give rise to the alternation of day and night as well as seasonal variation. By synchronizing their internal physiology with these recurring cycles, organisms align sleep–wake patterns, feeding behavior, and metabolic activity with the external environment, thereby maintaining temporal homeostasis. (Van Drunen & Eckel-Mahan, 2021). To synchronize with environmental cues, organisms rely on internal biological clocks that regulate diverse physiological functions. Two major endogenous rhythms are circadian (~24 h) and circannual (~1 year), both sustained without external stimuli and coordinated by central and peripheral clocks (Ayyar & Sukumaran, 2021).

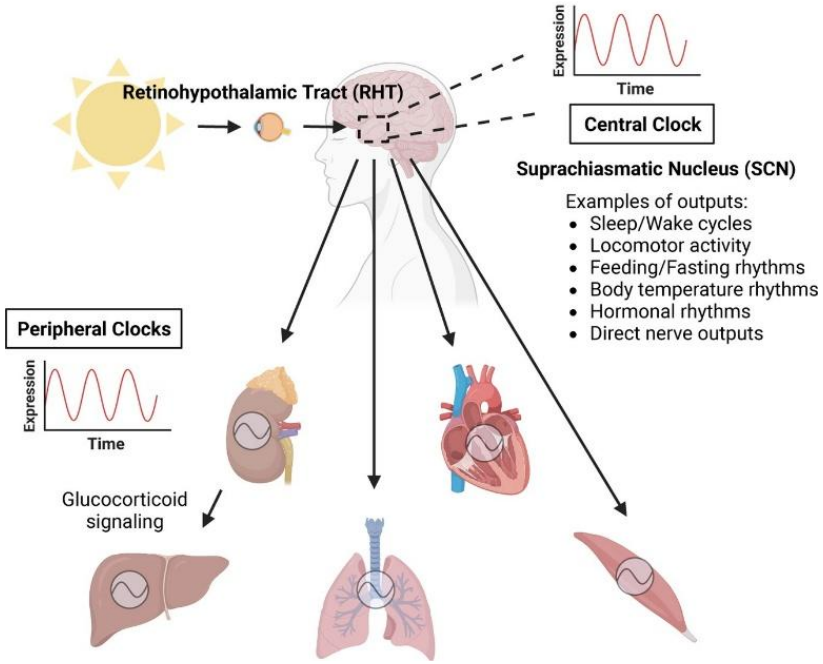

Figure 1. Central and peripheral clocks in mammals. The SCN receives light input via the RHT and synchronizes clocks in peripheral organs. Adapted from (Laothamatas et al., 2023).

In mammals, the central circadian clock resides in the suprachiasmatic nucleus (SCN) of the hypothalamus, which first aligns itself to the external light/dark cycle, the main environmental cue, or zeitgeber (ZT), through direct photic input from the retina. Once synchronized, the SCN subsequently entrains peripheral clocks via humoral signals and autonomic nervous activity, as illustrated in **Figure 1**. These peripheral oscillators, present in tissues such as liver, adipose tissue, and skeletal muscle, sustain their own rhythms and regulate organ-specific functions (Laothamatas et al., 2023). While coordinated by the SCN, they can also be entrained by external cues such as feeding, which act as ZT for peripheral clocks and independently modulate metabolism.

Circadian rhythms

As explained above, circadian rhythms are endogenous biological processes with a periodicity of approximately 24 hours. Found across all domains of life, from bacteria to mammals, these rhythms highlight a deeply conserved evolutionary mechanism (Ince, 2022). However, not all biological rhythms are circadian; specific criteria must be met. They must persist with ~24-h periodicity even without external cues, be entrainable by environmental signals to align with seasonal and geographical changes, and show temperature compensation, maintaining a stable period despite temperature fluctuations. (Narasimamurthy & Virshup, 2017).

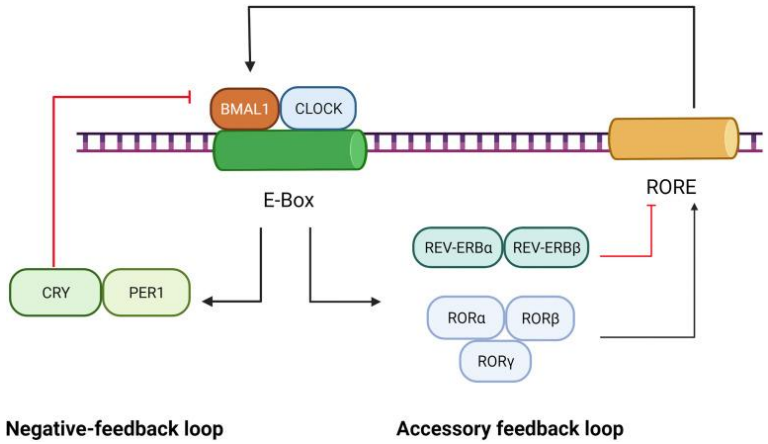

Figure 2. Schematic representation of the molecular circadian clock. The core loop involves CLOCK and BMAL1, which drive Per and Cry transcription via E-box elements, while PER/CRY complexes inhibit CLOCK:BMAL1 activity. An accessory loop regulates Clock and Bmal1 through RORs (activators) and REV-ERBs (repressors) acting on RORE sites. Obtained from (W. Zhang et al., 2022).

Circadian rhythms are generated by cell-autonomous molecular clocks based on interconnected feedback loops, as seen **Figure 2**. The core transcriptional negative-feedback loop (TNFL) involves circadian locomotor output cycles kaput

(*Clock*) and brain and muscle ARNT-like protein-1 (*Bmal1*), which form heterodimers that activate period (*Per*) and cryptochrome (*Cry*) genes through E-box elements. The resulting PER/CRY complexes inhibit CLOCK:BMAL1 activity, creating a self-sustained rhythm. An accessory loop regulates *Clock* and *Bmal1* expression through the action of both positive regulators, such as retinoic acid receptor-related orphan receptors (RORα, RORβ, and RORγ), and negative regulators, such as reverse erythroblastosis virus α and β (REV-ERBα and REV-ERBβ). These factors compete at ROR response elements (ROREs) to maintain rhythmic gene expression (W. Zhang et al., 2022). The CLOCK:BMAL1 complex regulates many clock-controlled genes, including *Nampt*, the rate-limiting enzyme in NAD^+ biosynthesis. Consequently, NAD^+ levels oscillate and modulate SIRT1 activity, which depends on the NAD^+/NADH ratio. Through this mechanism, SIRT1 regulates PER2 acetylation and the PER–CRY complex, ultimately feeding back on BMAL1 transcription (Soni et al., 2021).

Circadian disruption

As circadian rhythms are crucial for maintaining physiological balance, their deregulation can lead to a condition known as circadian disruption, which refers to the misalignment between internal biological rhythms and external environmental cues. According to Fishbein and colleagues, this disruption can result from factors such as shift work, jet lag, or exposure to artificial light at night, and is increasingly recognized as a risk factor for a variety of adverse health outcomes, including metabolic disorders, cardiovascular disease, behavioral disturbances, and even cancer (Fishbein et al., 2021). A key contributor to these adverse outcomes is oxidative stress. Recent studies highlight that the redox set point is not fixed but rather a variable, moving target value (Lim et al., 2022). This property is modulated by the circadian rhythm, which governs the daily oscillations of antioxidant defenses, and by external factors such as nutrition and exercise (McClean & Davison, 2022; Sies, 2021). This dynamic regulation suggests a bidirectional interplay between circadian and redox systems, therefore potentially offering mechanistic insight into the development of chronodisruption and its associated health outcome.

Oxidative stress

Oxidative stress is a disturbance in redox homeostasis caused by an imbalance between reactive species production and elimination, leading to

excess free radicals. These highly reactive molecules contain at least one unpaired electron, with reactive oxygen species (ROS) being the most relevant in biology. Elevated ROS can damage DNA, proteins, and membranes, triggering functional impairment, genomic instability, and cellular senescence or apoptosis (Juan et al., 2021). Oxidative stress is also a key driver of metabolic-associated fatty liver disease, mainly through lipid peroxidation, mitochondrial dysfunction, and chronic inflammation, which promote hepatocellular injury and disease progression (Arroyave-Ospina et al., 2021).

While high levels of free radicals are harmful, low to moderate concentrations are essential for redox balance, transcriptional regulation, and normal cell function. To maintain this balance, cells rely on a coordinated antioxidant system, including enzymes such as superoxide dismutases (SODs), catalase, and glutathione peroxidases (GPXs), along with small-molecule antioxidants that collectively protect against ROS-induced damage (Jomova et al., 2023).

In situations of oxidative stress, the antioxidant defense system may become insufficient. To reinforce cellular protection, additional pathways are activated, most notably those regulated by nuclear factor erythroid 2–related factor 2 (NRF2), which represents the master regulator of the cellular antioxidant response. Under normal conditions, NRF2 is sequestered in the cytoplasm by Kelch-like ECH-associated protein 1 (KEAP1). When ROS levels increase, specific cysteine residues in KEAP1 become oxidized, disrupting its ability to inhibit NRF2. This allows NRF2 to accumulate, translocate to the nucleus, and bind to antioxidant response elements (AREs), where it activates the transcription of genes involved in redox balance and cytoprotection. The key steps of this pathway are summarized in **Figure 3**.

As noted, the NRF2–KEAP1 sensing system resides in the cytoplasm but is unevenly distributed; a fraction localizes to the mitochondrial outer membrane, where its proximity to ROS production sites enables rapid detection and antioxidant activation (Wende et al., 2016). This localization is especially relevant because mitochondrial metabolism is the primary intracellular source of ROS, produced as byproducts of electron transport during nutrient oxidation (Wang et al., 2023). In addition to activating cytosolic defenses like NRF2, mitochondria employ intrinsic strategies such as dynamic network remodeling to limit oxidative damage and preserve homeostasis.

Mitochondrial dynamics

Mitochondria continuously undergo fusion and fission, processes collectively known as mitochondrial dynamics, essential for maintaining their morphology, distribution, and functionality. Fusion is a two-step, GTP-dependent process in which the outer mitochondrial membrane is merged by mitofusin 1 and 2 (MFN1/2) and the inner membrane by optic atrophy protein 1 (OPA1). This energy-consuming remodeling enables content exchange between mitochondria, diluting damaged components, supporting mitochondrial DNA maintenance, and sustaining optimal oxidative phosphorylation. It acts both as a homeostatic mechanism to preserve bioenergetic efficiency and as a salvage pathway to restore function to impaired organelles, helping the network adapt to metabolic demands and stress (S. Gao & Hu, 2021). Conversely, fission is a GTP-dependent process primarily driven by dynamin-related protein 1 (DRP1), which is recruited from the cytosol to the outer mitochondrial membrane by adaptors such as mitochondrial fission factor (MFF). Once assembled into constrictive spirals, DRP1 hydrolyzes GTP to sever the organelle, generating separate mitochondrial units. Functionally, fission supports normal organelle distribution, facilitates proliferation, and acts as a quality-control mechanism by isolating damaged segments for removal through mitophagy, particularly under stress or apoptotic conditions (Zerihun et al., 2023). A representation of both fusion and fission processes can be seen in **Figure 4**.

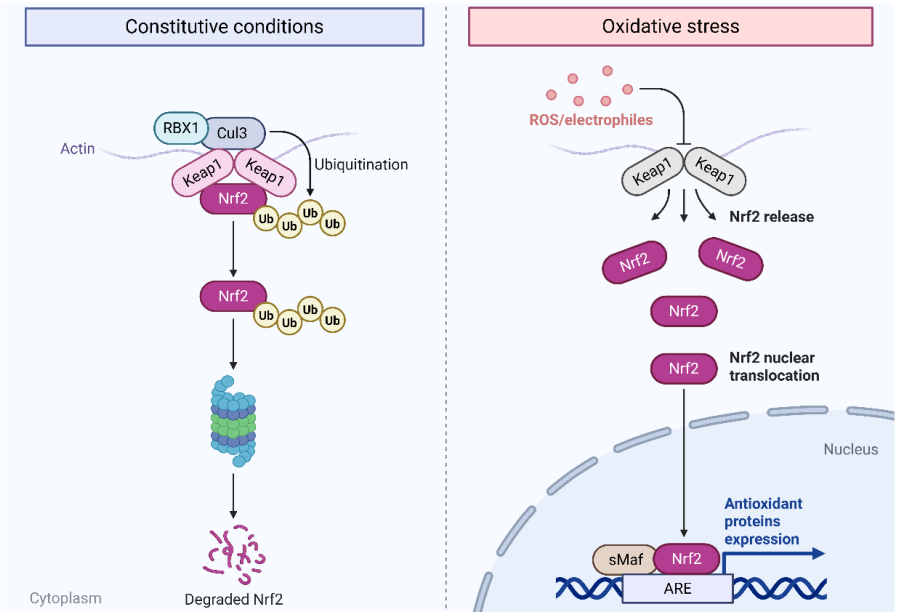

Figure 3. The NRF2 pathway under basal and oxidative stress conditions. Under normal conditions, NRF2 is ubiquitinated by the KEAP1–Cul3–RBX1 complex and degraded. During oxidative stress, KEAP1 is

inactivated, allowing NRF2 to accumulate, translocate to the nucleus, and activate antioxidant and cytoprotective genes. Adapted from (Bayo Jimenez et al., 2022).

Mitochondrial dynamics have a direct impact on oxidative stress regulation. Elevated ROS levels, if not counterbalanced by antioxidant defenses, promote mitochondrial fragmentation through increased fission and reduced fusion, leading to impaired bioenergetics and redox imbalance. Conversely, maintaining a balanced fusion, fission cycle supports mitochondrial quality control, optimizes respiratory efficiency, and sustains cellular redox homeostasis (Brillo et al., 2021). Therefore, there exists a clear bidirectional interplay between mitochondrial dynamics and oxidative stress, in which alterations in one process can directly influence and reinforce changes in the other.

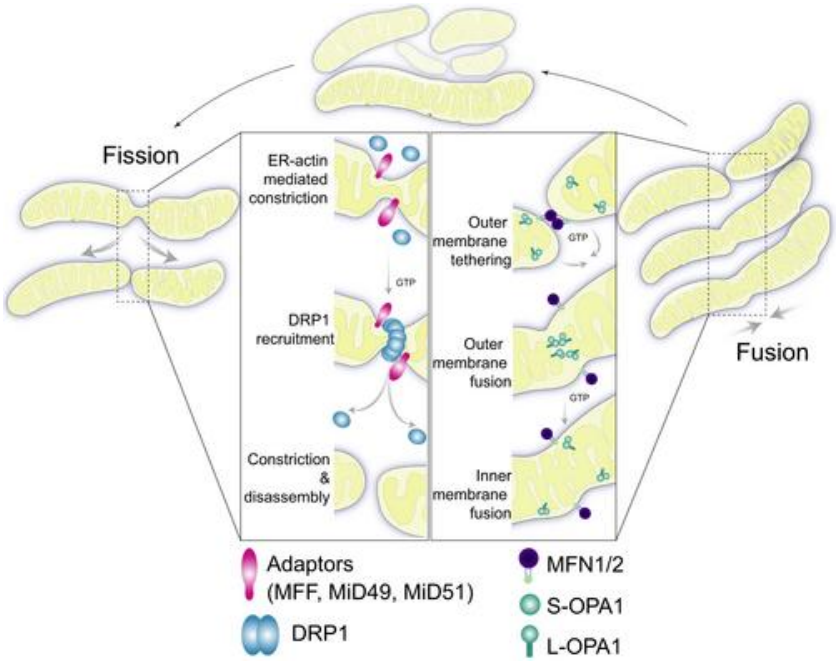

Figure 4. Fission begins at endoplasmic reticulum contact sites, where adaptor proteins recruit DRP1 to constrict and divide the organelle. Fusion requires outer membrane tethering by MFN1/2 followed by inner membrane fusion mediated by OPA1. Both processes are GTP-dependent and crucial for maintaining mitochondrial morphology and function. Obtained from (Yapa et al., 2021).

Relation between circadian rhythms and oxidative stress

Recent studies have shown that the circadian clock exerts a crucial role in maintaining redox homeostasis by regulating both the generation and detoxification of ROS. Several antioxidant genes, including those encoding catalase and enzymes involved in hydrogen peroxide metabolism, are under direct circadian regulation. For instance, overexpression of the core clock component BMAL1 has been shown to increase the mRNA and protein levels of SOD and NRF2, an effect associated with reduced ROS levels, thereby linking circadian control of antioxidant pathways to the maintenance of cellular

homeostasis (Chhunchha et al., 2020). Consistently, a study investigating the interplay between the NRF2 and NF-κB pathways and the circadian clock found that clock-synchronized cells mount a faster and more effective antioxidant response, limiting damage under chronic inflammatory conditions compared to desynchronized cells (W. Gao et al., 2022). Thus, desynchronized cells exhibit impaired antioxidant defenses and are more vulnerable to oxidative damage.

Relation between circadian rhythms and mitochondrial dynamics

The circadian clock tightly regulates mitochondrial morphology, which undergoes rhythmic shifts between tubular and fragmented forms. In healthy cells, these oscillations align with light–dark cycles, whereas disruption of core clock genes, such as BMAL1, abolishes rhythmicity, leading to larger, rounder mitochondria that maintain a constant shape throughout the day and night (Jin et al., 2023). Few studies have assessed daily oscillations in mitochondrial function, but rat brain mitochondria show a higher respiratory control ratio during the active phase, indicating more efficient coupling (Wende et al., 2016).

Overall, the circadian clock exerts tight control over both oxidative stress responses and mitochondrial dynamics. By regulating pathways such as NRF2/ARE, clock components coordinate the expression of antioxidant proteins to match daily fluctuations in oxidative load. In parallel, core clock genes and associated mediators, including calcineurin, AMPK, and sirtuins, orchestrate rhythmic cycles of mitochondrial fusion, fission, and quality control. Together, these mechanisms align mitochondrial morphology, function, and antioxidant defenses with metabolic and environmental demands across the day–night cycle.

Disruption of circadian rhythmicity, whether from lifestyle factors, environmental stressors, or disease, can weaken antioxidant defenses and destabilize mitochondrial function. Sleep deprivation, for example, promotes ROS accumulation through increased mitochondrial ATP production, endoplasmic reticulum stress, and oxidative protein folding, while persistent loss of sleep elevates ROS in peripheral organs, driving inflammation, DNA damage, and disease risk (Zeng et al., 2024). Similarly, disruption or mutation of clock genes abolishes the rhythmicity of mitochondrial dynamics, as seen in liver-specific BMAL1 knockout mice, which display altered lipid profiles, reduced OXPHOS protein and complex I levels, and enlarged, static mitochondria. These changes are associated with insulin resistance, lipotoxicity, excessive mitochondrial ROS,

Ca^{2+} mishandling, reduced membrane potential, impaired mitophagy, and ER stress (Jin et al., 2023). As seen in **Figure 5**, the circadian clock, redox homeostasis, and mitochondrial dynamics are tightly interconnected, and restoring rhythmic control has become a key therapeutic target.

One promising approach to restoring rhythmic control involves nutritional interventions, particularly the use of phytochemicals, within the framework of xenohormesis. In recent decades, evidence has shown that dietary components can influence internal biological clocks. For example, Cui and colleagues reported that a high-fat diet disrupts circadian rhythms, whereas supplementation with an apple (poly)phenol extract not only mitigated these disruptions but also improved metabolic health (Cui et al., 2022). (Poly)phenols, a diverse group of plant-derived secondary metabolites, have therefore gained attention for their capacity to modulate clock gene expression while supporting redox homeostasis.

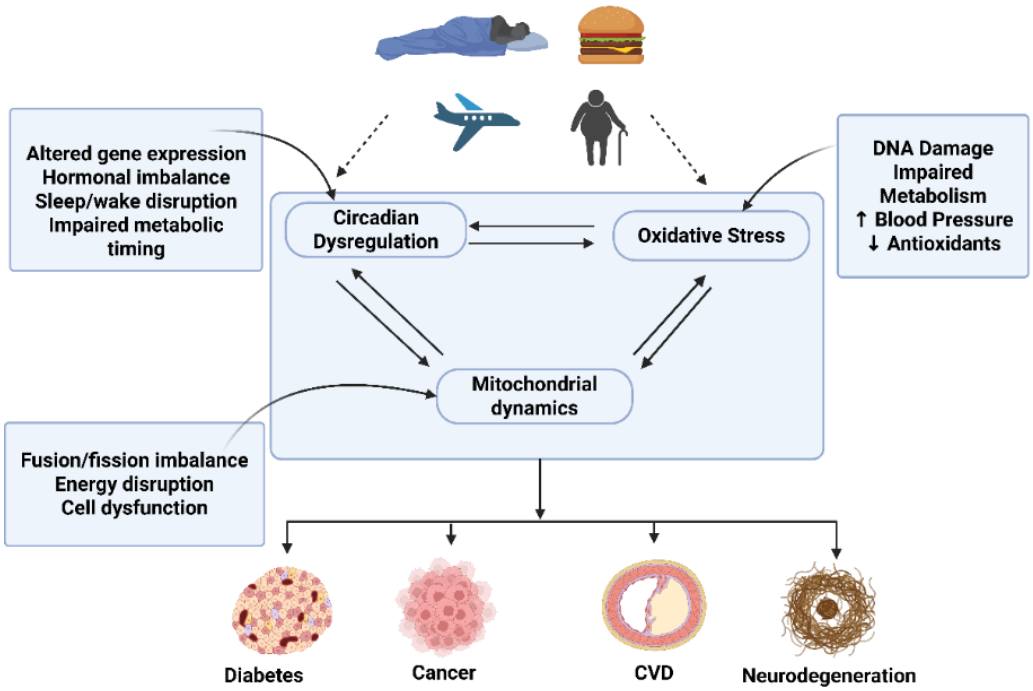

Figure 5. Schematic representation of the interplay between circadian dysregulation, oxidative stress, and mitochondrial dynamics. External factors such as aging, jet lag, sleep loss, or poor diet can disrupt circadian clocks, promoting oxidative stress and altered mitochondrial fusion/fission balance. These processes contribute to impaired metabolism, DNA damage, and increased risk of chronic diseases including diabetes, cancer, cardiovascular disorders, and neurodegeneration. Adapted from (McClean & Davison, 2022).

Phenolic compounds

Phenolic compounds constitute a large and diverse class of plant metabolites, within which (poly)phenols are the most abundant and widely studied group. (Poly)phenols are plant secondary metabolites, meaning they are not essential

for basic survival but contribute significantly to plant adaptation as they play important roles in plant fitness, including the attraction of pollinators, defense against oxidative stress, or protection against external harmful factors (Sharma et al., 2019). Beyond their importance for plant survival, (poly)phenols have attracted significant attention due to their potential health benefits in humans. Several studies highlight their antioxidant, anti-inflammatory, and mitochondrial-protective properties (Rajha et al., 2022). (Poly)phenols are broadly classified into flavonoids, phenolic acids, stilbenes, and lignans, with flavonoids further divided into subgroups such as flavanols, flavonols or flavones (Lang et al., 2024). Among flavanols, proanthocyanidins are of particular interest due to their high antioxidant capacity, and grape seed (poly)phenol extract (GSPE) is one of the richest natural sources of these compounds.

From a biotechnological standpoint, GSPE is relevant as it derives from grape pomace, a wine and juice by-product rich in phenolic compounds with antioxidant, antimicrobial, and anticancer properties. Its use supports waste valorization and a circular economy by converting residues into bioactive ingredients for nutraceutical, pharmaceutical, and food applications (Moselhy et al., 2023). In this regard, the Nutrigenomics Research Group of the URV have demonstrated that GSPE enhanced antioxidant defenses and reduced ROS levels in the liver of healthy and diet-induced obese rats exposed to an abrupt photoperiod change, therefore showing that GSPE elicits differential responses depending on the biological rhythms and circadian context (Cortés-Espinar et al., 2023). Furthermore, the same group has shown that GSPE modulated mitochondrial dynamics in the liver by enhancing the expression of fusion-related genes and reducing fission-related ones, with these effects being more pronounced when the extract was administered at night, thereby suggesting that the beneficial impact of GSPE on mitochondrial homeostasis is closely linked to circadian timing (Rodríguez et al., 2022). These findings highlight the potential of (poly)phenols, particularly GSPE, as modulators of oxidative stress, mitochondrial function, and circadian regulation.

Hypothesis and objectives

As chronodisruption alters the rhythmic expression of the genes involved in mitochondrial dynamics and oxidative stress, which lead to impaired antioxidant

defenses, we hypothesize that the supplementation with grape seed (poly)phenol extract (GSPE), which has been demonstrated to restore the diurnal rhythmicity of antioxidant-related genes as well as the genes related to mitochondrial dynamics, could partially restore or modulate these circadian patterns by attenuating the transcriptional repression of antioxidant pathways and by supporting mitochondrial function, thereby improving the adaptation to oxidative stress under disrupted photoperiods.

Therefore, the main objective was to evaluate the effects of chronodisruption and GSPE supplementation on feeding behavior, core clock gene expression, and the circadian regulation of mitochondrial dynamics and oxidative stress–related genes, to assess how (poly)phenols modulate physiological rhythms and antioxidant defenses under altered photoperiods. To address this aim, we defined the following specific objectives:

- To assess feeding patterns across experimental groups to determine how chronodisruption alters daily physiological rhythms and to justify subsequent molecular analyses of circadian regulation.
- To quantify and compare transcriptional levels of key clock, mitochondrial dynamics, and oxidative stress response genes under normal and disrupted photoperiods, with and without GSPE supplementation..
- To determine whether these genes exhibit diurnal rhythmic expression in each condition and evaluate how chronodisruption and GSPE influence the maintenance, loss, or induction of rhythmicity.
- To explore transcriptional correlations among clock, mitochondrial, and antioxidant genes, identifying functionally coherent modules (e.g. *Nrf2*–*Keap1*) and their potential coordination with circadian control.
- To compare the effects of chronodisruption and GSPE on behavioral, mitochondrial, antioxidant, and clock networks, identifying shared temporal windows of vulnerability or adaptation (e.g., ZT15–ZT21, rest-to-wake transition).

Materials and methods.

Grape Seed (Poly)phenol Extract (GSPE)

GSPE, derived from white grape seeds and skins, was supplied by Les Dérives Résiniques et Terpéniques (Dax, France). The phenolic profile of the

extract used in this study has been previously characterized by Nutrigenomics Research group (Arreaza-Gil et al., 2023), was mainly composed of catechin, epicatechin, and oligomeric procyanidins, specifically dimers, trimers, and tetramers, as well as epicatechin gallate, among other compounds.

Animals and Experimental Procedure

The experiment lasted five weeks, during which rats were maintained under their respective photoperiods and treatments. Sixty-four 12-week-old male Wistar rats (n = 64) were housed under controlled environmental conditions (22 ± 2 °C, 55 ± 10% humidity) with free access to food and water. All animals received a standard rodent diet (Envigo T.2014.12). Two different photoperiod regimens were applied: a 24-h cycle of 12 h light/12 h dark (L12) and a 22-h cycle of 11 h light/11 h dark (L11), the latter mimicking circadian disruption. Animals also received a daily oral dose of vehicle (VH) or GSPE. Prior to the intervention, all rats underwent a one-week adaptation period under their assigned photoperiod. Rats were then randomly distributed into four experimental groups (*n* = 16 per group) based on photoperiod and treatment: 1) L12 + VH (control photoperiod + vehicle), (2) L12 + GSPE (control photoperiod + GSPE), (3) L11 + VH (disrupted photoperiod + vehicle), and (4) L11 + GSPE (disrupted photoperiod + GSPE). To assess circadian rhythmicity, animals were euthanized at four ZT (3, 9, 15, and 21; *n* = 4 per time point per group) during the final day of the intervention. Euthanasia was carried out three hours after the last dose by decapitation. Tissues were immediately collected, frozen in liquid nitrogen, and stored at −80 °C until analysis. The experimental design is summarized in **Figure 6**.

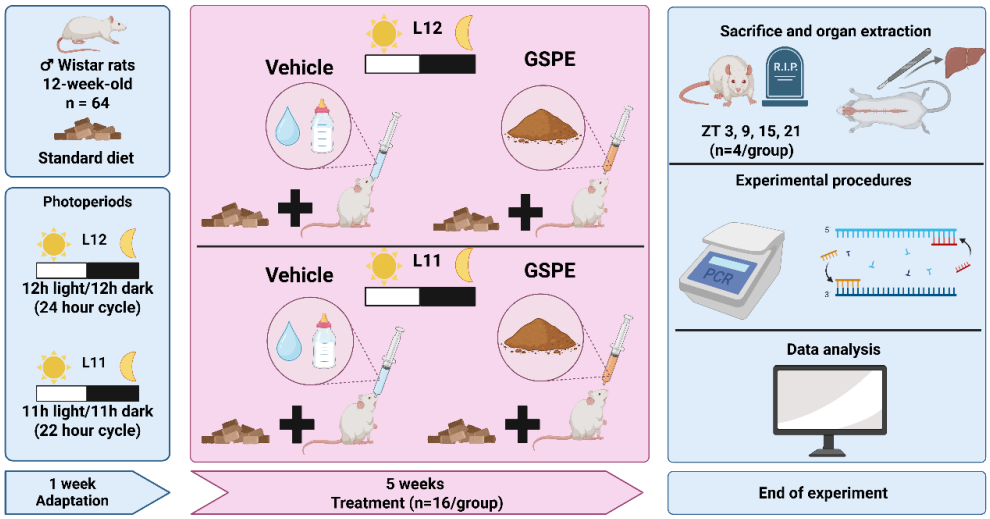

Figure 6. Experimental design. Sixty-four 12-week-old male Wistar rats were randomly distributed into four experimental groups (n = 16/group) according to photoperiod (12 h light/dark or 11 h light/dark) and treatment

(VH or GSPE [25 mg/kg/day]). After one week of adaptation to the assigned photoperiod, rats received the corresponding treatment by oral syringe administration for five weeks. At the end of the intervention, animals were euthanized at four zeitgeber times (ZT 3, 9, 15, and 21; n = 4 per ZT per group) for sample collection.

Dosage Information/Dosage Regimen

During the five weeks of the intervention, rats received a daily oral dose of either VH (condensed milk diluted in water, 1:5 v/v) or GSPE diluted in VH (25 mg/kg body weight). A GSPE dose of 25 mg/kg per day has been identified as the lowest effective amount capable of modulating a broad range of central metabolic pathways in healthy rats (Aragonès et al., 2016). This corresponds to an estimated human intake of ~370 mg of phenols per day, a level that can be readily achieved through (poly)phenol-rich dietary patterns such as the Mediterranean diet, after applying the standard rat-to-human conversion (Reagan-Shaw et al., 2008). Treatments were given once daily, two hours after lights-off, corresponding to ZT14 in L12 and ZT13 in L11.

Hepatic RNA Extraction

Total RNA was extracted from 20–30 mg of frozen liver tissue using Trizol® reagent (Thermo Fisher, Madrid, Spain) according to the manufacturer's instructions. Samples were homogenized with a TissueLyser LT device (Qiagen, Madrid, Spain), and the lysate was centrifuged at 12,000×g for 10 min at 4 °C. The supernatant was transferred to a clean tube, and 250 µL of chloroform was added. After centrifugation for 15 min at 12,000×g and 4 °C, the aqueous phase was collected and mixed with 500 µL of isopropanol, followed by a 10 min centrifugation at the same speed and temperature. The resulting RNA pellet was washed twice with 70% ethanol and centrifuged for 5 min at 8000×g (4 °C). Finally, the pellet was air-dried and resuspended in 60 µL of nuclease-free water. RNA concentration and purity were determined using a NanoDrop 1000 spectrophotometer (Thermo Scientific, Wilmington, DE, USA).

cDNA Synthesis

Complementary DNA (cDNA) was synthesized from total RNA using the High-Capacity cDNA Reverse Transcription Kit (Applied Biosystems, Barcelona, Spain), following the manufacturer's protocol. The reverse transcription reaction was performed in a Galaxy XP ClearLine thermal cycler (ClearLine, Dominique Dutscher, Brumath, France).

Quantitative PCR (qPCR) was carried out using Quantitative PCR (qPCR) was carried out using NZYSupreme qPCR Green Master Mix (2×) (NZYTech,

Lisbon, Portugal) in a QuantStudio™ 5 Real-Time PCR System, 384-well format (Thermo Fisher Scientific, Waltham, MA, USA). Primer sequences for the target genes are listed in Table 1 and were synthesized by Biomers.net (Ulm, Germany).

Table 1. Nucleotide sequences of primers used for RT-qPCR.

Gene	Accession Number	Forward Primer (5' to 3')	Reverse Primer (5' to 3')
Cry1	NM_198750.2	*TGGAGGGTATGCGTGTCCTC*	*TCCAGGAGAACCTCCTCACG*
Bmal1	*NM_024362.2*	GTAGATCAGAGGGCGACGGCTA	CTTGTCTGTAAAACTTGCCTGTGAC
Nampt	*NM_177928.3*	*CTCTTCACAAGAGACTGCCG*	*TTCATGGTCTTTCCCCCACG*
Rorα	*NM_001427367.2*	*CCCGATGTCTTCAAATCCTTAGG*	*TCAGTCAGATGCATAGAACACAA ACTC*
Sirt1	*NM_001414959.1*	*TTGGCACCGATCCTCGAA*	*ACAGAAACCCCAGCTCCA*
Clock	*NM_001389254.1*	*TGGGGTCTATGCTTCCTGGT*	*GTAGGTTTCCAGTCCTGTCG*
Per2	*NM_031678.2*	*CGGACCTGGCTTCAGTTCAT*	*AGGATCCAAGAACGGCACAG*
Ppia	NM_017101.1	TCAAACACAAATGGTTCCCAGT	ATTCCTGGACCCAAAACGCT
Sod1	NM_017050.1	GGTGGTCCACGAGAAACAAG	CAATCACACCACAAGCCAAG
Sod2	NM_017051.2	AAGGAGCAAGGTCGCTTACA	ACACATCAATCCCCAGCAGT
Catalase	NM_012520.2	GAATGGCTATGGCTCACACA	CAAGTTTTTGATGCCCTGGT
GPx1	NM_030826.4	TGCAATCAGTTCGGACATC	CACCTCGCACTTCTCAAACA
Gsr	NM_053906.2	ATCAAGGAGAAGCGGGATG	GCGTAGCCGTGGATGACT
Mfn1	NM_138976.2	CCTTGTACATCGATTCCTGGGTTC	CCTGGGCTGCATTATCTGGTG
Pcg1a	NM_031347.1	AGAGTCACCAAATGACCCCAAG	TTGGCTTTATGAGGAGGAGTCG
Drp1	NM_001437697.1	CCAGGAATGACCAAGGTCCC	CCTCGTCCATCAGGTCCAAC
Mfn2	NM_130894.5	GATGTCACCACGGAGCTGGA	AGAGACGCTCACTCACTTTG
Fis1	NM_001401051.1	GCACGCAGTTTGAATACGCC	CTGCTCCTCTTTGCTACCTTTGG

Gene-Expression Analysis

To evaluate primer efficiency, a pooled cDNA sample was generated by mixing 1 µL of cDNA from each of 16 randomly selected samples (total volume: 16 µL). This pool was then diluted 1:10 by adding 144 µL of nuclease-free water. Serial dilutions of 1:20, 1:40, and 1:80 were prepared by mixing 80 µL of the previous dilution with 80 µL of water, yielding 160 µL per point. All RT-qPCR reactions for efficiency assessment were performed using these dilutions.

Primer efficiency was calculated individually for each gene included in the study, which comprised mitochondrial dynamics-related genes, oxidative stress markers, and core clock genes (see **Table 1** for the complete list of targets and primer sequences). Reactions were run in technical triplicates, and Ct values from each dilution were used to construct standard curves. Amplification efficiency (E) was calculated using the formula $E = 10^{(-1/\text{slope})}$. Only genes with efficiencies close to 2 (100%) were considered acceptable for further analysis. All calculations were performed using Microsoft Excel custom spreadsheets.

For experimental samples, each RT-qPCR reaction was performed in a final volume of 5 µL per well using 384-well plates. The reaction mix consisted of 3 µL of master mix prepared in a 2.5:0.25:0.25 ratio of SYBR Green, forward primer, and reverse primer, respectively, and 2 µL of diluted cDNA (1:10). Plates were sealed with optical adhesive film, briefly centrifuged, and loaded into the

QuantStudio™ 5 system for amplification, following the manufacturer's instructions for the qPCR master mix.

Relative mRNA expression levels were calculated using the $2^{-\Delta\Delta Ct}$ method, with Peptidylprolyl Isomerase A (*Ppia*) as the endogenous control, as described by (Livak & Schmittgen, 2001). Results were expressed as fold changes relative to the L12-VH group at ZT3 (Rodríguez et al., 2022)

Analysis of Diurnal Rhythmicity

Diurnal rhythmicity in gene and protein expression was assessed using a Cosinor-based approach, which fits oscillatory models and estimates MESOR (mean level of oscillation), amplitude (peak–MESOR distance), and acrophase (timing of the peak).A custom script was developed in Python (v.3.7.4; Wilmington, DE, USA) using PyCharm software (v.2018.2.4; JetBrains s.r.o., Prague, Czech Republic) by J.R. S-R. Analyses were performed with the CosinorPy package (v.1.1; Ljubljana, Slovenia) (Moškon, 2020). Rhythmicity was considered significant when the cosine model provided a fit with $p < 0.05$. Methods were adapted from Cortés-Espinar and colleagues and Rodríguez and collaborators (Cortés-Espinar et al., 2023; Rodríguez et al., 2022).

Determination of AOX Activities in Liver Tissue

Liver samples were homogenized in cold phosphate buffer (50 mM, pH 7.0) at a ratio of 0.5 g of tissue per 4.5 mL of buffer, using an Ultra-Turrax T25 homogenizer (IKA, Staufen, Germany). From each homogenate, 400 µL were extracted and immediately mixed with 400 µL of 12% metaphosphoric acid for subsequent glutathione determination, while the remaining homogenate was centrifuged at 1000 rpm for 10 min at 4 °C. The resulting supernatant was collected and aliquoted into 1.5 mL microcentrifuge tubes (aiming for ~600 µL per sample) for thiol group analysis.

GSH (glutathione) content was determined as described by Griffith and colleagues (Griffith, 1980). Deproteinized samples were neutralized with phosphate–EDTA buffer, incubated with NADPH and DTNB, and treated with glutathione reductase (50 U/mL) to keep GSH reduced. Absorbance was recorded at 412 nm (Hitachi U-1900), and total glutathione (GSH + GSSG) was quantified from a standard curve.

Protein thiol content was determined following the method described by Jocelyn (Jocelyn, 1987). Supernatants were diluted 1:20 in phosphate–EDTA

buffer (20 mM/1 mM, pH 8) and incubated in semi-micro cuvettes. Absorbance at 412 nm was recorded before and after adding Ellman's reagent (DTNB, 10 mM). Thiol content was calculated from a BSA calibration curve and expressed as nmol –SH/mg protein.

Statistical analysis

All analyses were performed using R version 4.5.1 and RStudio version 2025.05.1-513. The distribution and homogeneity of the variables were assessed using the Shapiro–Wilk and Levene's tests, respectively. Since several variables did not meet the assumptions of normality or homoscedasticity, all subsequent analyses were performed using non-parametric tests to ensure a conservative and uniform approach across datasets.

Differences in fold changes from RT-qPCR data and liver ROS parameters (n = 4 per group and ZT) were analyzed using the aligned rank transform (ART), a non-parametric approach that enables factorial analyses with standard ANOVA procedures. Unlike traditional non-parametric tests such as Kruskal–Wallis or Scheirer–Ray–Hare, which are limited to main effects and cannot properly evaluate interactions, the ART preserves the ability to test both main and interaction effects while avoiding assumptions of normality (Wobbrock et al., 2011). This makes it particularly suitable for our experimental design, where interaction effects between photoperiod and treatment were of primary interest. After alignment and ranking of the data, two-way ANOVAs were performed, followed by Tukey's post hoc tests for pairwise comparisons.

Correlations between gene expression levels were assessed in RStudio using Spearman's rank correlation coefficient (ρ). This method was selected because gene expression data may not follow a normal distribution and can be affected by outliers. As noted by Schober and colleagues, Spearman's correlation is more robust under these conditions than Pearson's correlation and is therefore well suited for biological datasets (Schober et al., 2018). Pairwise correlations were calculated, and significance was set at $p < 0.05$.

Repeated-measures variables, such as food intake during active and rest phases, were analyzed using the Friedman test, the non-parametric alternative to one-way repeated-measures ANOVA. This test is particularly suitable when data violate the assumptions of parametric models, as it relies on ranking within blocks and is robust to deviations from normality and homoscedasticity (Pereira

et al., 2015). All data are reported as mean ± SEM or median ± interquartile range (IQR), and statistical significance was considered at $p < 0.05$.

Results

Chronic disruption alters feeding behavior, leading to reduced intake

Initially, we examined the effects of diet and photoperiod on the animals' feeding pattern. As shown in **Figure 7A**, the altered photoperiod influenced nighttime, daytime, and total food intake. Nighttime intake differed between photoperiods throughout the intervention in both treatments; however, in the final week this effect disappeared in the vehicle groups and remained only between the L12–GSPE and L11–GSPE groups. Overall, non-disrupted animals consumed more per hour during the night. Daytime intake consistently varied between photoperiods in both treatments (**Figure 7B**), with chronodisrupted animals eating more per hour. Finally, total intake at the end of the intervention also showed a significant photoperiod effect in both treatments (**Figure 7C**), with chronodisrupted animals consuming less overall across the day.

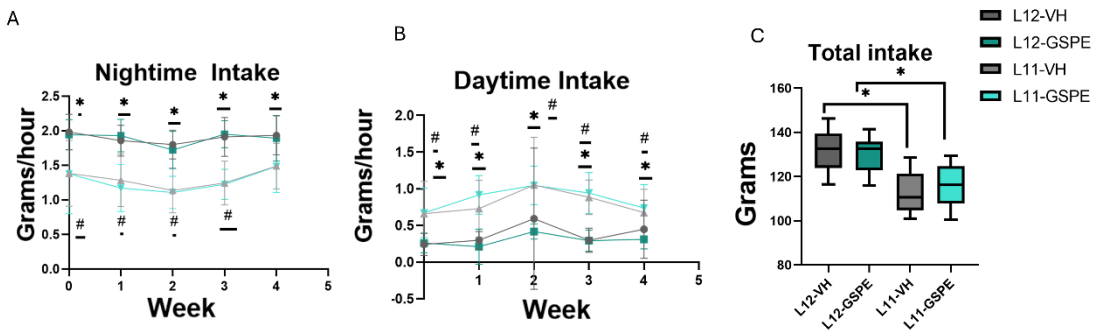

*Figure 7. Effect of diet and photoperiod on feeding behavior. (A) Nighttime food intake (g/hour) and (B) daytime food intake (g/hour) were measured weekly throughout the intervention (repeated measures). (C) Total food intake (g) was calculated at the end of the intervention. Data are presented as mean ± SEM (A, B) or median and interquartile range (IQR) (C). Groups: L12–VH, animals under a 12 h light–dark cycle receiving vehicle; L12–GSPE, 12 h light–dark cycle receiving grape seed proanthocyanidin extract (GSPE); L11–VH, 11 h light–dark cycle receiving vehicle; L11–GSPE, 11 h light–dark cycle receiving GSPE. In panels A and B: *p < 0.05 between L12–GSPE and L11–GSPE; #p < 0.05 between L12–VH and L11–VH. In panel C: *p < 0.05 indicates statistically significant differences between groups.*

Chronic Photoperiod Disruption Alters the Expression of Core Clock Genes

We next analyzed the expression of clock-related genes to evaluate whether photoperiod and GSPE influenced the molecular circadian machinery. As seen in **Figure 8**, both photoperiod and GSPE treatment clearly modulated the expression of clock genes. *Nampt* showed combined photoperiod and treatment effects at ZT15, with reduced expression in both L11–VH and L12–GSPE compared to L12–VH (**Figure 8A**). *Cry1* displayed a consistent photoperiod effect

across all ZTs, most notably at ZT15 and ZT21, where both treatments were affected by L11 (**Figure 8B**). *Rorα* exhibited time-dependent effects, with no differences detected at ZT21, but both photoperiod and treatment effects evident at ZT9 (**Figure 8C**). *Bmal1* showed a photoperiod effect in both treatments, limited to ZT3 (**Figure 8D**). In contrast, *Clock* expression remained stable across conditions, with no significant changes detected at any time point (**Figure 8E**). *Per2* displayed a modest photoperiod effect, with altered expression in L11–VH relative to L12–VH at ZT15 (**Figure 8F**). *Rev-erbα* was particularly sensitive, showing treatment effects at ZT3 and ZT21, with GSPE supplementation reducing expression relative to vehicle (**Figure 8G**). Finally, *Sirt1* showed a photoperiod effect at ZT21, with higher expression in L12–VH compared to L11–VH, and a similar trend observed in the GSPE groups (**Figure 8H**).

Having shown that both factors affected several clock genes, we next evaluated their diurnal rhythmicity under 24 h (L12) and 22 h (L11) cycles. As shown in **Figure 8I**, all genes were rhythmic in at least one group. *Nampt* and *Per2* were rhythmic across all conditions, whereas *Bmal1* only under L11 and Sirt1 only in L12–VH and L11–GSPE. Overall, some genes maintained rhythmicity in all groups, while others displayed group-specific patterns.

Following clock gene rhythmicity analysis, we evaluated correlations among their expression profiles. As shown in **Figure 9**, *Per2* correlated positively with *Cry1* and *Bmal1*, while *Cry1* also associated with *Clock* and *Reverb-α*. Negative correlations were observed between *Rorα* and *Bmal1*, and between *Reverb-α* and *Sirt1*. These results highlight coordinated regulation within the clock machinery. Full correlation data, including p-values, rho coefficients, and FDR adjustments, are provided in the appendix (**Supplementary Table 1**).

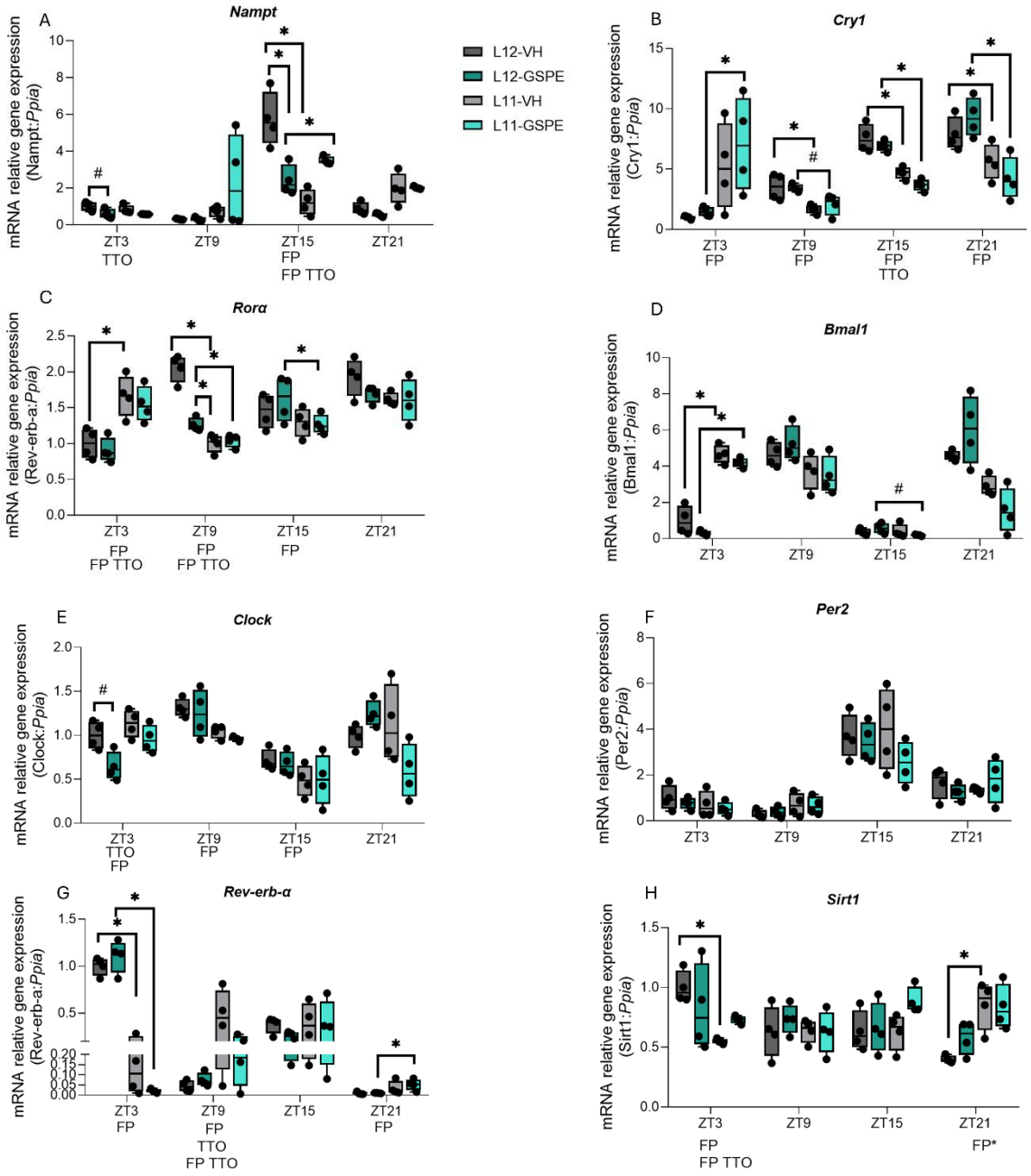

I

Gene	L12-VH	L12-GSPE	L11-VH	L11-GSPE
NAMPT	✓	✓	✓	✓
CRY1	✓	✓	✓	⊘
RORa	⊘	✓	✓	✓
BMAL1	⊘	⊘	✓	✓
CLOCK	✓	⊘	✓	✓
PER2	✓	✓	✓	✓
REVERBa	✓	✓	✓	✓
SIRT1	✓	⊘	⊘	✓

Figure 8. Effects of photoperiod shortening and GSPE supplementation on clock-gene expression. (A–H) Relative mRNA levels of Nampt, Cry1, Rorα, Bmal1, Clock, Per2, Rev-erbα, and Sirt1 at ZT3, ZT9, ZT15, and ZT21. Data are presented as box plots of gene expression normalized to Ppia; points represent

*individual animals. *p < 0.05; #trend (p < 0.1). (I) Summary table showing the presence (green check marks) or absence (red crossed symbols) of diurnal rhythmicity for the expression of each gene in the experimental groups (L12–VH, L12–GSPE, L11–VH, L11–GSPE), as determined by cosinor analysis.*

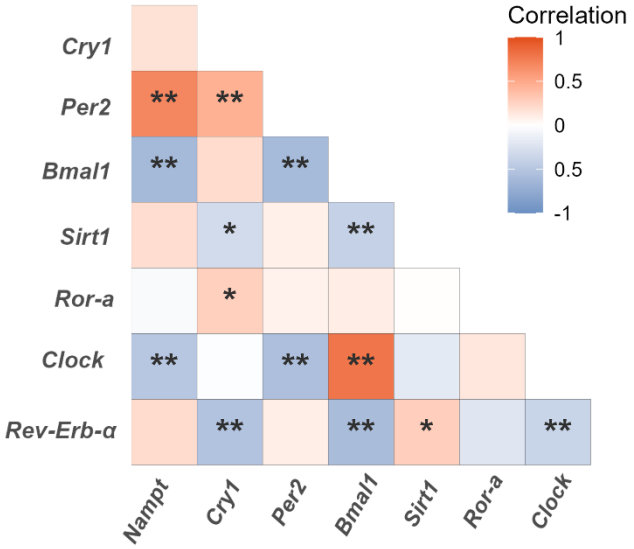

*Figure 9 Correlation matrix of clock gene expression. Pearson's coefficients are shown, with positive correlations in red, negative in blue, and color intensity indicating strength. *p < 0.05, **p < 0.01.*

Oxidative stress pathways are transcriptionally affected by chronic disruption

We next assessed oxidative stress–related transcripts (**Figure 10)**. *Sod1* displayed a photoperiod effect at ZT3, an interaction at ZT15, and a treatment effect at ZT21 (**Figure 10A**). *Sod2* showed multiple effects at ZT15 (treatment, photoperiod, and interaction) and additional differences at ZT21 (**Figure 10B**). *GPx1* exhibited a significant interaction at ZT3 **(Figure 10C**). *Keap1* differed at ZT3 due to treatment and at ZT9 owing to an FP-Treatment interaction (**Figure 10D**). *Nrf2* expression remained stable, with no significant changes across groups or time points (**Figure 10E**). In contrast, *Gsr* exhibited a treatment effect at ZT21, with reduced levels in GSPE-supplemented animals relative to vehicle (**Figure 10F**). Finally, *Catalase* displayed a photoperiod effect at ZT21, with higher expression in L12–VH than in L11–VH, a pattern attenuated by GSPE (**Figure 10G**). Taken together, oxidative stress genes showed time-dependent and gene-specific sensitivities to photoperiod and GSPE.

To assess diurnal rhythmicity in oxidative-stress genes, we evaluated the L12 (24-h) and L11 (22-h) groups. As shown in **Figure 10H**, rhythmicity was gene- and group-specific: *Sod1* expression did not exhibit significant rhythmicity in any of the groups; *Sod2* was rhythmic only in L12–GSPE; *Gpx1* displayed rhythmicity in L12–GSPE and L11–GSPE; in contrast, *Gsr* and *Nrf2* did not show detectable rhythmicity under any condition; *Keap1* and *Catalase* exhibited rhythmicity only

in L11–GSPE. Taken together, rhythms were present for a subset of targets and varied by group.

After rhythmicity analysis, we examined co-expression among oxidative-stress genes. As seen in **Figure 11**, most correlations were positive, with *Nrf2* and *Keap1* showing significant associations with several antioxidant targets, including *Sod1*. *Catalase* correlated positively with *Sod1* and *GPx1*. Only one significant negative correlation was observed (*Nrf2–Gsr*). Full correlation values are provided in (**Supplementary Table 2**).

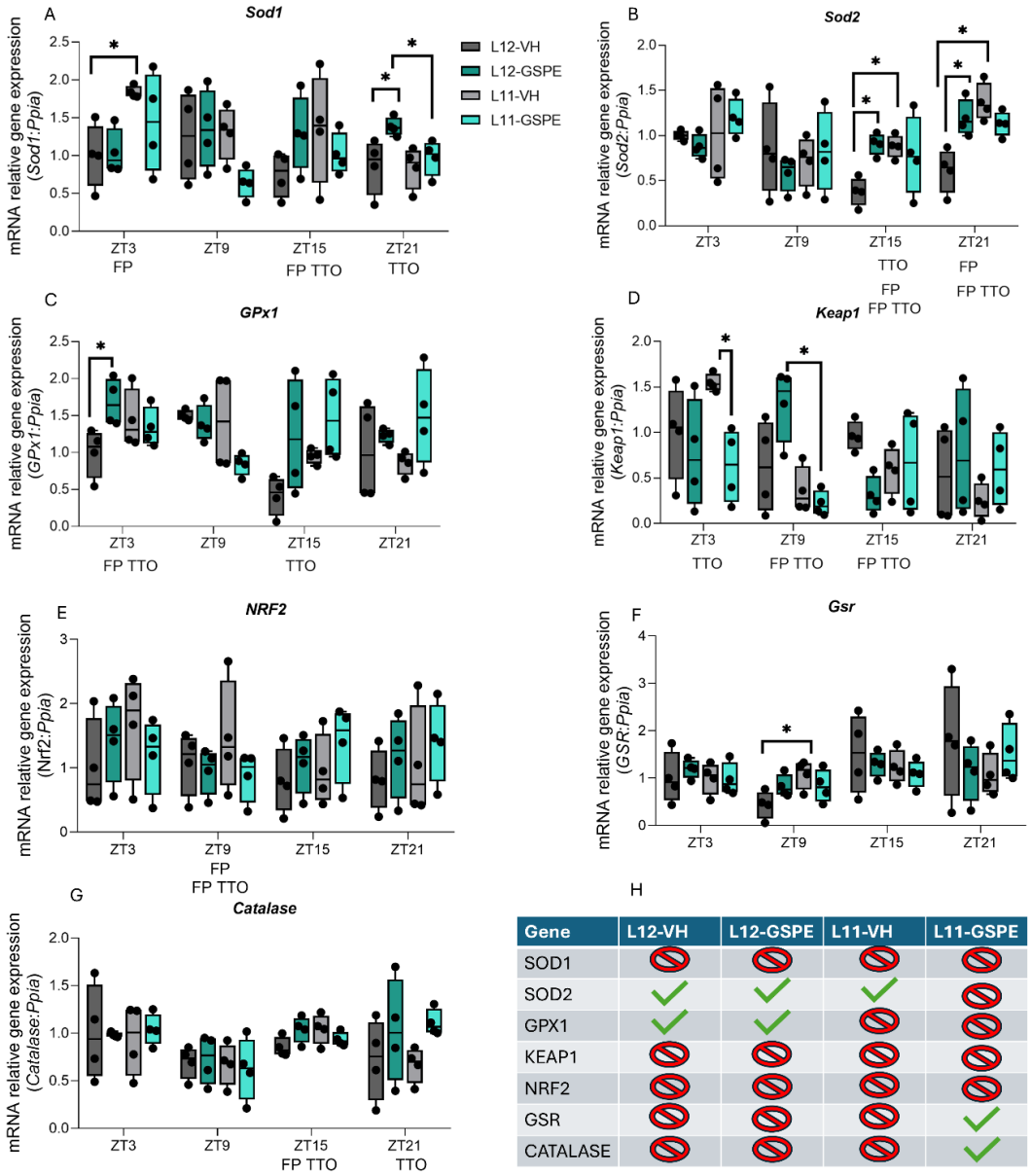

Gene	L12-VH	L12-GSPE	L11-VH	L11-GSPE
SOD1	⊘	⊘	⊘	⊘
SOD2	✓	✓	✓	⊘
GPX1	✓	✓	⊘	⊘
KEAP1	⊘	⊘	⊘	⊘
NRF2	⊘	⊘	⊘	⊘
GSR	⊘	⊘	⊘	✓
CATALASE	⊘	⊘	⊘	✓

*Figure 10. Effects of photoperiod shortening and GSPE supplementation on oxidative stress–related gene expression. (A–G) Relative mRNA levels of Sod1, Sod2, Gpx1, Keap1, Nrf2, Gsr, and Catalase at ZT3, ZT9, ZT15, and ZT21. Data are presented as box plots of gene expression normalized to Ppia; points represent individual animals. *p < 0.05; #trend (p < 0.1). (H) Summary table showing the presence (green check marks) or absence (red crossed symbols) of diurnal rhythmicity for the expression of each gene in the experimental groups (L12–VH, L12–GSPE, L11–VH, L11–GSPE), as determined by cosinor analysis.*

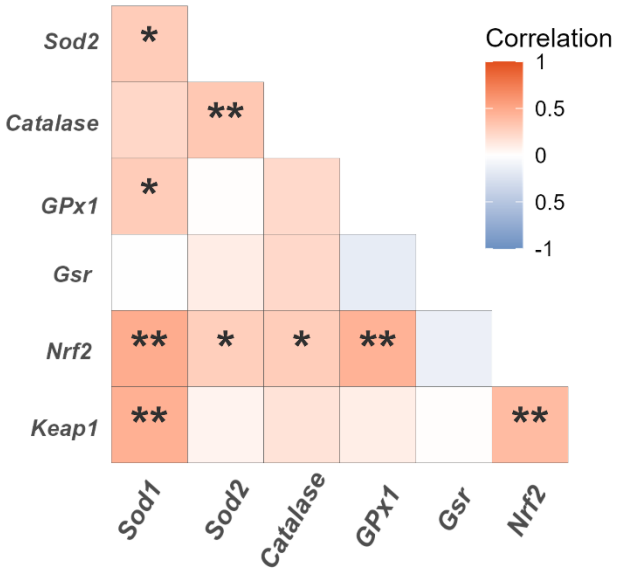

*Figure 11. Correlation matrix of oxidative stress–related gene expression. Pairwise Pearson correlations (r) among relative mRNA levels of Sod1, Catalase, Gpx1, Gsr, Nrf2, and Keap1. Positive correlations are shown in red and negative in blue; color intensity reflects magnitude (−1 to +1). Asterisks denote significance: *p < 0.05; **p < 0.01.*

Having examined the expression profile of antioxidant genes, we sought to determine whether the observed alterations could exert any significant effect on hepatic ROS levels. To this end, we evaluated the concentrations of thiols and glutathione (GSH). As shown in **Figure 12**, thiols (–SH groups) displayed treatment-specific effects at distinct ZTs. At ZT3, GSPE significantly reduced thiol levels in L12, whereas at ZT15 and ZT21, the reduction was observed in L11. In contrast, no significant differences in GSH levels were detected between groups at any ZT.

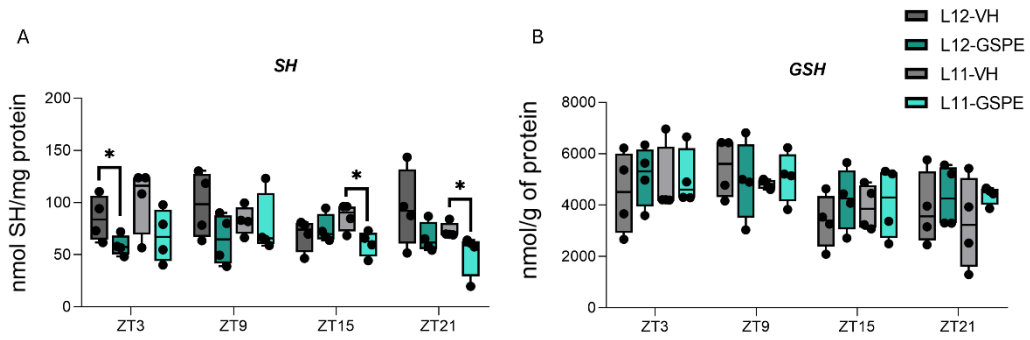

*Figure 12. Hepatic thiol and glutathione levels across different ZTs. (A) Total thiols (–SH groups) expressed as nmol SH/mg protein. GSPE significantly reduced thiol levels at ZT3 in L12 and at ZT15 and ZT21 in L11. (B) Glutathione (GSH) levels expressed as nmol/g protein. No significant differences were observed between groups at any ZT. Data are represented as box plots with individual values (n = 4 per group). *p < 0.05.*

Circadian disruption leads to transcriptional alterations in mitochondrial dynamics

We then assessed the expression of genes involved in mitochondrial dynamics. As shown in **Figure 13**, several genes displayed time- and group-specific differences. *Mfn1* showed a photoperiod effect at ZT15 as its expression

was lower in L11–VH than L12–VH, with a similar trend between L11–GSPE and L12–GSPE (**Figure 13A**). *Mfn2* exhibited a treatment effect within the 22-h cycle at ZT21, with L11–GSPE reduced relative to L11–VH (**Figure 13B**). *Fis1* displayed a photoperiod effect within the GSPE groups at ZT15, with L11–GSPE showing lower levels than L12–GSPE (**Figure 13C**). *Pgc1α* showed multiple differences at ZT15 and ZT21 involving both photoperiod and treatment (**Figure 13D**). In addition, *Drp1* expression displayed a strong photoperiod effect at ZT21, with higher expression in L11–VH compared to L12–VH, a difference attenuated by GSPE supplementation (**Figure 13E**) Taken together, these data show gene-specific modulation of mitochondrial fusion, fission, and biogenesis markers.

To assess diurnal rhythmicity in mitochondrial-dynamics genes, we evaluated the L12 (24-h) and L11 (22-h) groups. As shown in **Figure 13F**, rhythmicity was gene- and group-specific: *Mfn1* was rhythmic only in L12–VH; *Mfn2* was rhythmic in L12–GSPE and L11–VH; *Pgc1α* showed rhythmicity in both L12 groups but not under L11; *Drp1* was rhythmic only in L11–GSPE; and *Fis1* only in L11–VH. Overall, some rhythms were confined to the 24-h cycle (e.g., *Pgc1α*), others to the 22-h cycle (e.g., *Fis1*, *Drp1*), while MFN2 appeared in both.

After the rhythmicity analysis, we evaluated co-expression among mitochondrial-dynamics genes. As shown in **Figure 14**, correlations were predominantly positive. The strongest association was between *Pgc1α* and Mfn2 ($p < 0.01$), and *Fis1* also correlated positively with *Mfn2* ($p < 0.05$). No other pairwise correlations reached significance, including those involving *Drp1* or *Mfn1*. Overall, significant associations clustered around *Mfn2*. The full set of correlation values, including p-values, rho coefficients, and FDR-adjusted significance levels for all comparisons, is provided in the appendix (**Supplementary Table 3**).

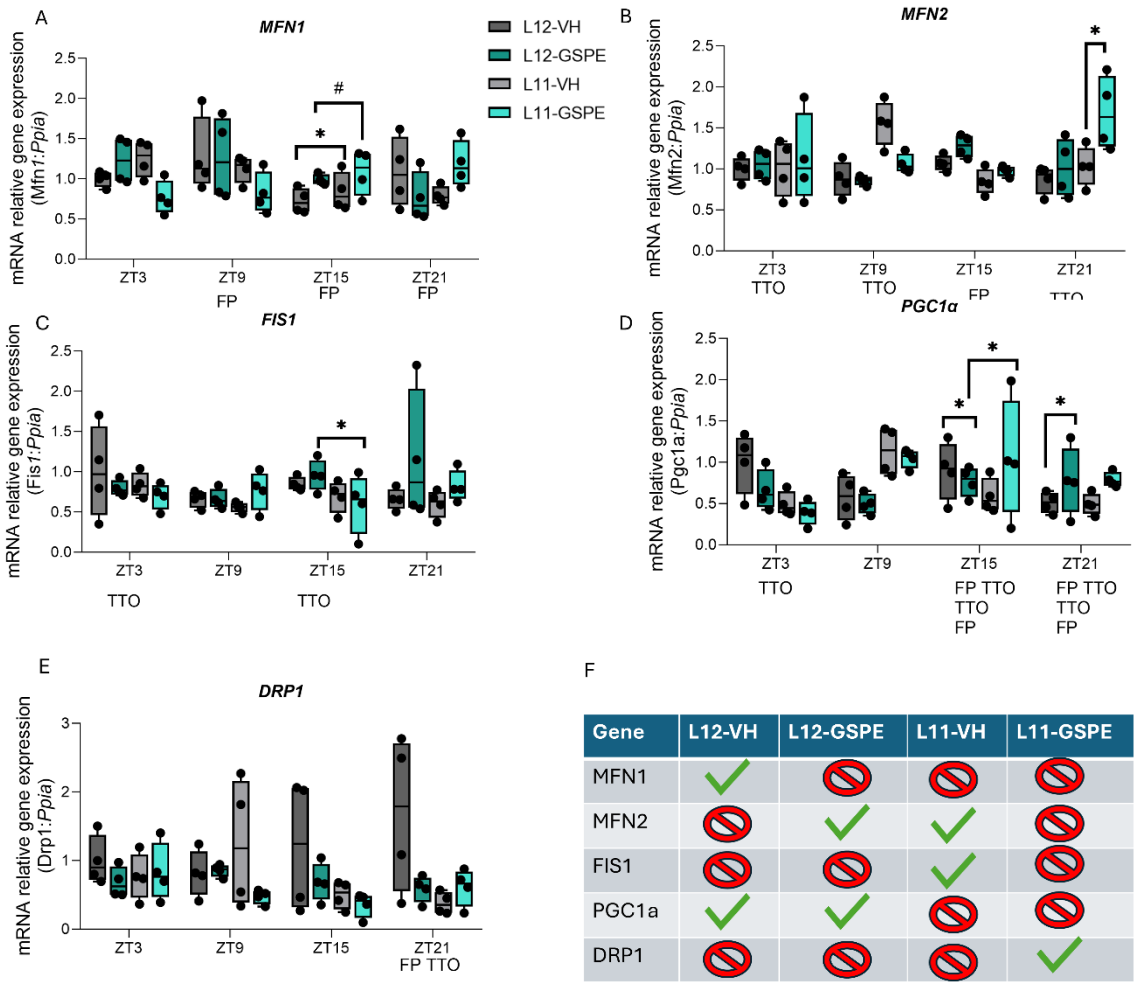

*Figure 13. Effects of photoperiod shortening and GSPE supplementation on genes involved in mitochondrial dynamics and biogenesis. (A–E) Relative mRNA levels of Mfn1, Mfn2, Fis1, Pgc1α, and Drp1 at ZT3, ZT9, ZT15, and ZT21. Data are presented as box plots of gene expression normalized to Ppia; points represent individual animals. *p < 0.05; #trend (p < 0.1). (F) Summary table showing the presence (green check marks) or absence (red crossed symbols) of diurnal rhythmicity for the expression of each gene in the experimental groups (L12–VH, L12–GSPE, L11–VH, L11–GSPE), as determined by cosinor analysis. Abbreviations: GSPE, grape-seed (poly)phenol extract; VH, vehicle; L12, 12 h light/12 h dark; L11, 11 h light/11 h dark; ZT, zeitgeber time.*

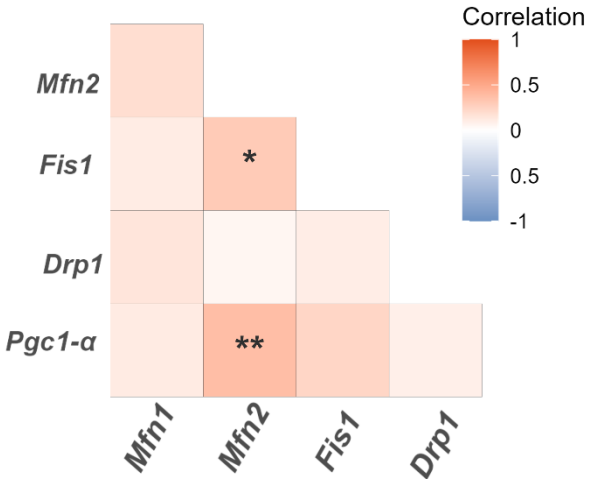

*Figure 14. Correlation matrix of mitochondrial-dynamics gene expression. Pairwise Pearson correlations (r) among relative mRNA levels of Mfn1, Mfn2, Fis1, Drp1, and Pgc1α. Positive correlations are shown in red and negative correlations in blue; color intensity reflects magnitude (scale −1 to +1). Asterisks indicate statistical significance: *p < 0.05; **p < 0.01.*

Discussion

In this study, the effects of chronic chronodisruption, induced by shortening the light–dark cycle of rats from 24 to 22 hours, and its potential mitigation by GSPE consumption were evaluated. Chronodisruption was found to alter the molecular clock machinery and associated pathways, while GSPE supplementation partially counteracted these effects. Recent studies further support the 22-h photoperiod model (T22) as a reliable approach to induce circadian disruption. For instance, Pugliane and collaborators reported that adolescent rats exposed to T22 displayed dissociation of locomotor rhythms together with deficits in recognition memory (Pugliane et al., 2025). Similarly, Schwartz and colleagues showed that rats under T22 develop two distinct bouts of activity due to weak coupling between suprachiasmatic nucleus subregions, leading to altered free-running periods (Schwartz et al., 2022). Altogether, these findings highlight the T22 paradigm as a relevant tool to investigate chronic circadian misalignment.

To assess the effects of chronic chronodisruption, feeding behavior was first compared during daytime, nighttime, and across the total cycle. Nighttime intake was characterized by a higher hourly food consumption in the non-disrupted groups compared to the chronodisrupted ones (**Figure 7A**). During daytime, the opposite pattern was observed: chronodisrupted animals consumed more food per hour than the non-disrupted groups (**Figure 7B**). Across the experiment, the differences between disrupted and non-disrupted groups tended to diminish, but this effect was only evident during nighttime intake, their active phase. This is reflected in the loss of significance between the vehicle groups in the final week, suggesting that disrupted animals were progressively adapting to the new light conditions. Interestingly, this convergence was not observed in the GSPE-supplemented groups, which maintained differences until the end of the intervention. However, since vehicle groups also retained differences in daytime intake, no clear conclusion regarding a modulatory role of GSPE on feeding behavior can be drawn. Nonetheless, the total food intake at the end of the experiment (**Figure 7C**) revealed that disrupted groups maintained a significant reduction compared to their non-disrupted counterparts. Therefore, despite the adaptive trend observed in feeding behavior, the outcome indicates that

chronodisrupted animals developed an altered feeding pattern, inconsistent with their natural physiology, which ultimately led to a reduced overall intake. These results are in line with previous evidence showing that circadian disruption alters feeding behavior. Meléndez-Fernández and colleagues described that exposure to artificial light at night and mistimed meals leads animals (and humans) to eat at abnormal times; for instance, rodent models exposed to light at night redistribute their food intake into the rest phase, even when total caloric intake may not differ, a pattern that disrupts circadian clocks and promotes metabolic dysfunction (Meléndez-Fernández et al., 2023). Similarly, Pickel & Sung synthesize many animal studies showing that when feeding rhythms are shifted (e.g., food restricted to the light phase in nocturnal rodents), animals eat during their usual resting period, which uncouples peripheral clocks from the SCN and impairs energy balance (Pickel & Sung, 2020). Consistent with these reports, our chronodisrupted animals also ate during the resting phase and, in addition, displayed a reduced total intake.

Following the evaluation of physiological parameters such as feeding behaviour, we analyzed the impact of chronodisruption on gene expression and the potential modulatory role of GSPE. In some cases, alterations were restricted to specific ZTs, whereas in others they were more consistent across the cycle. For instance, *Cry1* (**Figure 8B**) and *Rorα* (**Figure 8C**) displayed alterations across most ZTs.

A particularly notable response was observed at ZT15, where *Nampt* (**Figure 8A**) showed localized modulation: both treatments exhibited photoperiod-dependent differences, and an additional treatment effect was detected under L12 conditions. Although ZT15 does not exactly correspond to the rest-to-active transition (which occurs around ZT11–12), it is positioned close to this switch from the light/inactive phase to the dark/active phase. Such transitions represent critical windows of circadian regulation and are especially sensitive to disruption. Supporting this, a recent study reported that nearly half of the synaptic phosphoproteins in the mouse forebrain displayed large-amplitude rhythms peaking specifically at rest–activity and activity–rest transitions, underscoring the heightened vulnerability of these phase boundaries to circadian and sleep–wake perturbations (Brüning et al., 2019). By contrast, some genes such as *Clock* (**Figure 8E**) or *Per2* (**Figure 8F**) showed no significant changes, suggesting that

chronodisruption does not exert a uniform effect across the molecular clockwork. Instead, its impact appears selective, with certain genes (e.g., *Cry1* and *Rorα*) being consistently altered while others remain largely unaffected.

In summary, the strongest effects were consistently attributed to chronodisruption, while GSPE exerted a more modest influence, suggesting a modulatory rather than corrective role. Even then, the modulatory impact observed was limited compared to prior reports, which have shown that (poly)phenols can alter clock gene expression patterns (Ávila-Román et al., 2021; Spaleniak & Cuendet, 2023). Thus, our findings appear to diverge from earlier studies. Notably, chronodisruption did not elicit a uniform transcriptional response: some genes, such as *Cry1* and *Rorα*, were consistently affected, whereas others, including *Clock* or *Sirt1*, remained largely unchanged. However, since the number of samples per time point was relatively limited, subtle changes in certain genes could have been missed due to reduced statistical power. Despite this limitation, the effects of chronodisruption were still clearly perceptible.

After determining the effects on gene expression, we next examined whether these genes maintained rhythmicity and, more importantly, whether they lost it or adapted to a 22-hour cycle. As shown in the results (**Figure 9I**), most genes displayed clear diurnal rhythmicity under L12 conditions, with some exceptions such as *Bmal1* and *Rorα* in the vehicle group. This does not imply that these genes are inherently arrhythmic; rather, under the specific conditions of our study and with the statistical program applied, significant rhythmicity could not be confirmed. Indeed, an extensive body of literature demonstrates that *Rorα* or *Bmal1* exhibit a robust and well-defined circadian rhythm (Lee, 2021; Z. Zhang et al., 2021).

Under L11 conditions (**Figure 8I**), it is noteworthy that, with few exceptions, such as *Sirt1* in the L11-VH group, all groups exhibited diurnal rhythmicity adjusted to a 22-hour cycle. This finding highlights the remarkable plasticity of the circadian system, as the transcriptional machinery appeared to adapt to the shortened cycle in order to synchronize physiology and behavior to the new environment, consistent with previous research (Boivin et al., 2022). Importantly, adaptation does not imply optimal clock performance. In our L11 animals, 22-h entrainment coexisted with altered expression profiles. Mechanistic work shows

that when the clock network is constrained, rhythmic outputs can be **partially** restored by available ZT (e.g., feeding), yet many programs remain suboptimal or require cross-tissue clock communication (Greco et al., 2021).

After determining the rhythmicity of clock genes, we next evaluated whether correlations existed between their expression profiles. As shown in **Figure 9**, several correlations emerged that had clear biological relevance. For instance, *Bmal1* was strongly and positively correlated with *Clock*, while showing negative correlations with *Per2*, *Nampt*, and *Sirt1*. This was expected: on one hand, *Bmal1* and *Clock* constitute the core activators of the transcriptional machinery, whereas *Per2* functions as a classical repressor within the negative feedback loop (Guan & Lazar, 2021). The negative correlations with *Nampt* and *Sirt1* are also consistent, since both genes are tightly linked to the metabolic regulation of the clock, modulating NAD^+ availability and deacetylation processes that ultimately reduce BMAL1 activity (Soni et al., 2021)

In line with this framework, additional correlations followed the same pattern: for example, *Per2* correlated positively with *Nampt*, and both in turn were positively associated with *Cry1*. This makes biological sense, as all three act as repressors or regulators that dampen the activity of the core CLOCK:BMAL1 complex, ensuring the oscillatory balance of the circadian machinery. Altogether, these results indicate that the correlation patterns observed in our study are both biologically coherent and in strong agreement with previous circadian research (Fagiani et al., 2022) .

Having examined the expression profile, rhythmicity, and correlations of core-clock genes, we proceeded to evaluate the same parameters in genes related to the oxidative stress response. As shown in the results, the expression profile reveals both clear effects of chronodisruption and GSPE treatment. For instance, *Sod1* (**Figure 10A**) shows higher transcriptional levels in L11-VH than in L12-VH at ZT3, as well as a treatment effect in L12 at ZT21. *GPx1* (**Figure 10C**) displays only a treatment effect in ZT3 between the L12 groups. Overall, chronodisruption exerts stronger effects than GSPE, consistent with the patterns already observed in mitochondrial dynamics and clock genes.

However, some findings are particularly noteworthy. For example, *Sod2* (**Figure 10B**) shows concurrent upregulation by both GSPE and chronodisruption at ZT15 and ZT21 compared to L12-VH. This is remarkable because it indicates

that the main impact of chronodisruption occurs during the transition from rest to wake and persists until ZT21, a phase when antioxidant responses appear to be exacerbated alongside peak animal activity. This observation is consistent with previous reports showing that ROS levels exhibit circadian rhythmicity, typically rising during the rest-to-wake transition in rodents. For example, glutathione levels in the rat heart have been shown to peak at the onset of the active phase, underscoring how antioxidant defenses are reinforced at this vulnerable time (Wende et al., 2016). Moreover, given that *SOD2* is the mitochondrial isoform (Zaidi et al., 2021), these results parallel our findings on mitochondrial dynamics, where the strongest alterations were also detected at ZT15 (**Figure 13).** This coincidence indicates a clear correlation between the altered antioxidant response and mitochondrial remodeling observed in our study, in line with previous evidence showing that circadian regulation of mitochondrial dynamics and antioxidant defense are closely interconnected (Mezhnina et al., 2022).

A similar pattern is seen with *Keap1* (**Figure 10D**), which is reduced in L11-GSPE at ZT3 and ZT9, suggesting an attenuation of chronodisruption-induced effects. This reduction may represent a GSPE-driven adaptation that enhances the oxidative stress response by lowering KEAP1, thereby facilitating NRF2 stabilization and nuclear translocation. Mechanistically, decreased KEAP1 would release more NRF2 from repression, preventing its degradation and enabling the transcription of antioxidant genes. Interestingly, *Nrf2* itself did not show significant transcriptional changes at any time point (**Figure 10E**), which aligns with previous reports where GSPE increased NRF2 activity without directly inducing its gene expression. In this regard, Nutrigenomics Research group had already shown that GSPE downregulated *Keap1* expression in CAF-fed rats (Cortés-Espinar et al., 2023), and our findings extend this evidence to the context of photoperiod-induced chronodisruption. Together, these results reinforce the notion that *Keap1* modulation could be a central mechanism of GSPE's action, although more research is needed to establish whether this pathway consistently explains its antioxidant effects.

In terms of diurnal rhythmicity, only a subset of oxidative stress genes exhibited oscillatory patterns (**Figure 10H**), and these were strongly dependent on the condition. *Sod2* showed rhythmic expression in all groups except L11-GSPE, suggesting that chronodisruption alone (L11-VH) preserves its rhythmicity,

while the combination with GSPE blunts it. *Sod1* and *GPx1* displayed rhythmicity exclusively under control photoperiod with GSPE (L12-GSPE), indicating that supplementation under normal conditions is capable of inducing or enhancing rhythmic oscillations. In contrast, *Catalase* exhibited rhythmicity only in L11-GSPE, suggesting that this enzyme responds specifically to the combination of chronodisruption and treatment. The remaining genes (*Gsr*, *Nrf2*, *Keap1*) did not show rhythmicity in any condition, highlighting their relative stability across photoperiods and treatments. Altogether, these data reveal that the antioxidant system is only partially rhythmic, with enzymes directly involved in ROS detoxification (SOD1, SOD2, GPX1, CATALASE) being more prone to circadian oscillations than regulatory components (NRF2, KEAP1). Interestingly, GSPE appears to shift rhythmicity patterns: it induces rhythmicity in certain genes under normal conditions (*Sod1, GPx1*) but abolishes it in others under disrupted conditions (*Sod2*), suggesting a complex, context-dependent modulation of antioxidant rhythms.

Curiously, there is clear evidence that connects the circadian clock with the Nrf2/ARE pathway. For example, under oxidative stress induced by renal ischemia–reperfusion, endogenous circadian genes, including BMAL1, were shown to regulate Nrf2, and disruption of this rhythmic control altered antioxidant protein expression and increased sensitivity to stress (Sun et al., 2021). Mechanistically, BMAL1 binds E-boxes in the Nrf2 promoter to drive its circadian oscillation and downstream antioxidant activity, while Nrf2 in turn enhances *Cry2* expression and represses CLOCK/BMAL1-driven transcription (W. Zhang et al., 2022). This bidirectional regulation, as seen in **Figure 15**, reveals that the circadian clock and the Nrf2/ARE pathway form an interconnected loop, integrating cellular redox signals into circadian timekeeping while simultaneously providing protection against oxidative, apoptotic, and inflammatory stress (W. Zhang et al., 2022).

Given this strong mechanistic link, it is not surprising that the lack of BMAL1 rhythmicity observed in our study (see above) coincided with the absence of Nrf2 oscillations and the generally weak diurnal rhythmicity of antioxidant genes. However, these observations should be interpreted with caution, since the limited sample size per time point (n=4) reduces statistical power, meaning that our

findings may reflect tendencies or predictions rather than definitive oscillatory patterns.

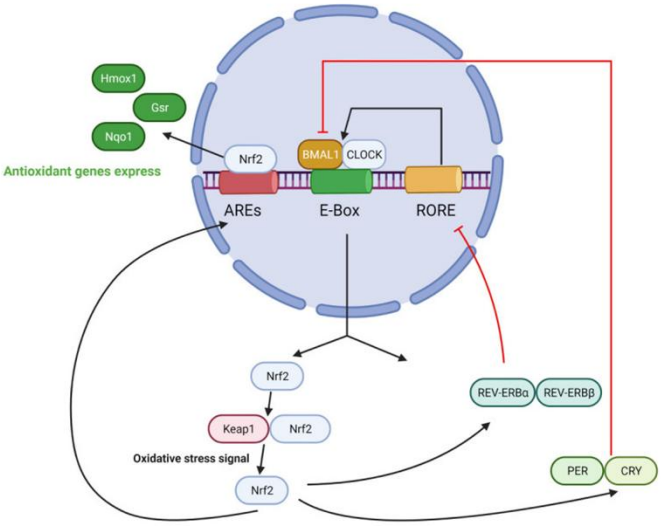

Figure 15. Simplified scheme illustrating the reciprocal regulation between circadian clock components and the Nrf2 pathway. The figure emphasizes the direct crosstalk, showing how Bmal1 promotes Nrf2 transcription and how Nrf2 feeds back by regulating Cry2 expression, thereby influencing Clock/Bmal1 activity. Adapted from (W. Zhang et al., 2022).

When analyzing correlations among oxidative stress genes, several strong and significant associations emerged (**Figure 11**). *Sod1* correlated positively with *Catalase*, suggesting a coordinated regulation between superoxide dismutation and hydrogen peroxide clearance. Likewise, *Catalase* displayed strong correlations with both *GPx1* and *Nrf2*, consistent with their shared role in peroxide detoxification and antioxidant defense (Wang et al., 2023).

Nrf2 emerged as a central hub, showing significant positive correlations with *GPx1*, *Catalase*, and *Keap1*, which reflects the classical regulatory axis where NRF2 activates downstream antioxidant enzymes and is itself negatively regulated by KEAP1 (Bayo Jimenez et al., 2022). Interestingly, the positive association with KEAP1 may indicate that their expression levels are co-modulated transcriptionally, even if their functional interaction is antagonistic at the protein level.

Keap1 also showed significant correlations with *Sod1* and *Nrf2*, reinforcing the idea that *Keap1* expression is functionally tied to the broader antioxidant response through its regulation of NRF2 and downstream antioxidant enzymes (Romero-Durán et al., 2024). In contrast, *Gsr* exhibited weaker or absent correlations with most genes, suggesting that glutathione regeneration may be regulated through distinct mechanisms not tightly coupled with the canonical

Nrf2-driven axis. This is consistent with its function: GSR acts to regenerate reduced glutathione and thereby replenishes antioxidant capacity, meaning it does not participate directly in the acute oxidative stress response but rather supports redox balance before and after stress events (Lai et al., 2021).

Following the analysis of the antioxidant gene profile, we examined whether hepatic ROS levels were altered (**Figure 12**). As described in the results, thiols exhibited treatment effects at several ZTs, whereas GSH levels remained unchanged. This indicates that chronodisruption does not follow a homogeneous route in ROS generation. Interestingly, thiol levels were reduced in disrupted rats under the influence of GSPE. Previous studies have consistently reported the antioxidant properties of GSPE (Marino et al., 2022; Rodriguez-Mateos et al., 2024); however, it is particularly noteworthy that this effect was restricted to ZT15 and ZT21. This pattern is recurrent throughout our study, as these ZTs correspond to the active phase of the animals, a period in which we also detected more pronounced alterations in the expression of antioxidant genes and in mitochondrial dynamics. In essence, GSPE appears to exert its impact precisely when antioxidant support is most required.

In contrast, during ZTs corresponding to the resting phase, no significant GSPE-mediated differences were observed, likely because antioxidant demand is not exacerbated by chronodisruption under a less catabolic state. Furthermore, as illustrated by GSH levels (**Figure 12B**), not all ROS-related parameters follow the same trend. For instance, as shown in **Figure 10C**, *GPx1* expression was minimally affected by either disruption or GSPE and remained unaltered during the wake phase. These findings suggest that chronodisruption does not induce a generalized increase in GSH-mediated antioxidant responses and therefore does not uniformly disrupt the antioxidant network.

Subsequent to the evaluation of antioxidant response genes, the same parameters were assessed in genes associated with mitochondrial dynamics. As shown in **Figure 13**, and in contrast to clock genes, only a few alterations were observed in response to either chronodisruption or GSPE treatment. Interestingly, most differences were located at ZT15, which, as discussed for the clock genes, represents a critical time point near the transition from the rest phase to the active phase. Specifically, *Mfn1* expression was higher in chronodisrupted animals compared to their non-disrupted counterparts, a result that is in line with the

downregulation observed for *Fis1* in L11-GSPE relative to L12-GSPE. Together, these findings suggest that chronodisruption may shift the fusion–fission balance towards fusion at the transition from rest to activity. In contrast, *Pgc1-α* showed a downregulation in L11-VH compared to L12-VH, while L11-GSPE tended to show an upregulation compared to L12-GSPE. However, the dispersion within the L11-GSPE group was too high to draw conclusive results. These results nonetheless point to a downregulation of one of the main transcription factors driving mitochondrial biogenesis under chronodisrupted conditions.

In essence, this creates an apparent contradiction between the evidence from *Mfn1/Fis1* and that from *Pgc1α*. In this regard, a prior study showed that *Bmal1* knockout mice present a downregulation of *Mfn1* and *Opa1* (Gabriel et al., 2021), suggesting that circadian disruption reduces mitochondrial fusion. Furthermore, a recent study describes *Pgc1α* as a key transcriptional co-activator of mitochondrial biogenesis that promotes fusion, particularly through robust induction of *Mfn2* (Chen et al., 2023). In contrast, the same work highlighted that ROS downregulate MFN1 at the protein level, thereby impairing the fusion machinery. In our study, the reduction of *Pgc1α*, together with the upregulation of antioxidant response genes, suggesting elevated ROS levels, provides convergent evidence that the fusion network was compromised. Altogether, these findings indicate that mitochondrial fusion was ultimately repressed rather than fission being enhanced. Nevertheless, further studies are needed to clarify whether chronodisruption promotes or represses mitochondrial fusion at the rest-to-activity transition, although the current data incline towards a repressive effect.

After analyzing the expression profiles, we evaluated the diurnal rhythmicity of mitochondrial dynamics genes and whether it was preserved under disrupted conditions (**Figure 13E**). Under normal conditions, most genes did not display rhythmicity, with a few exceptions such as *Mfn1* and *Pgc1α*, whose interplay has already been discussed. Interestingly, GSPE supplementation induced rhythmicity in *Mfn2*, further supporting previous reports of its ability to modulate the rhythmic expression of certain genes (Ávila-Román et al., 2021). Under chronodisrupted conditions, most genes similarly lacked rhythmicity, except for *Mfn2* and *Fis1*. Notably, *Drp1* also gained rhythmicity upon GSPE administration, suggesting that the treatment may influence certain nodes of the mitochondrial dynamics' machinery.

Altogether, our findings suggest that mitochondrial dynamics are not primarily driven by rhythmic gene expression but instead rely on post-translational regulation. Indeed, several studies have demonstrated that circadian control of mitochondrial morphology relies heavily on post-translational mechanisms. For example, calcineurin activity follows a daily rhythm, promoting the dephosphorylation of DRP1 at Ser637 and its translocation to the mitochondrial membrane (Huang et al., 2012) . CLOCK can also modulate DRP1 by inhibiting the stabilizing factor PUF60, thereby increasing DRP1 abundance when its activity is compromised (Xu et al., 2022). AMPK, whose activation is clock-dependent, further connects energy status to mitochondrial remodeling: it promotes fission and mitophagy during energy stress, enhances fusion via *Mfn2* upregulation during fasting, and influences circadian timing by phosphorylating PER2 and CRY. Additionally, sirtuins integrate mitochondrial and circadian regulation: SIRT1 interacts with CLOCK–BMAL1 to regulate PER2 stability, while SIRT3 ensures OPA1 deacetylation and fusion maintenance under stress through the NAD^+/SIRT axis (Jin et al., 2023). A schematic summary of these mechanisms is presented in **Figure 16.**

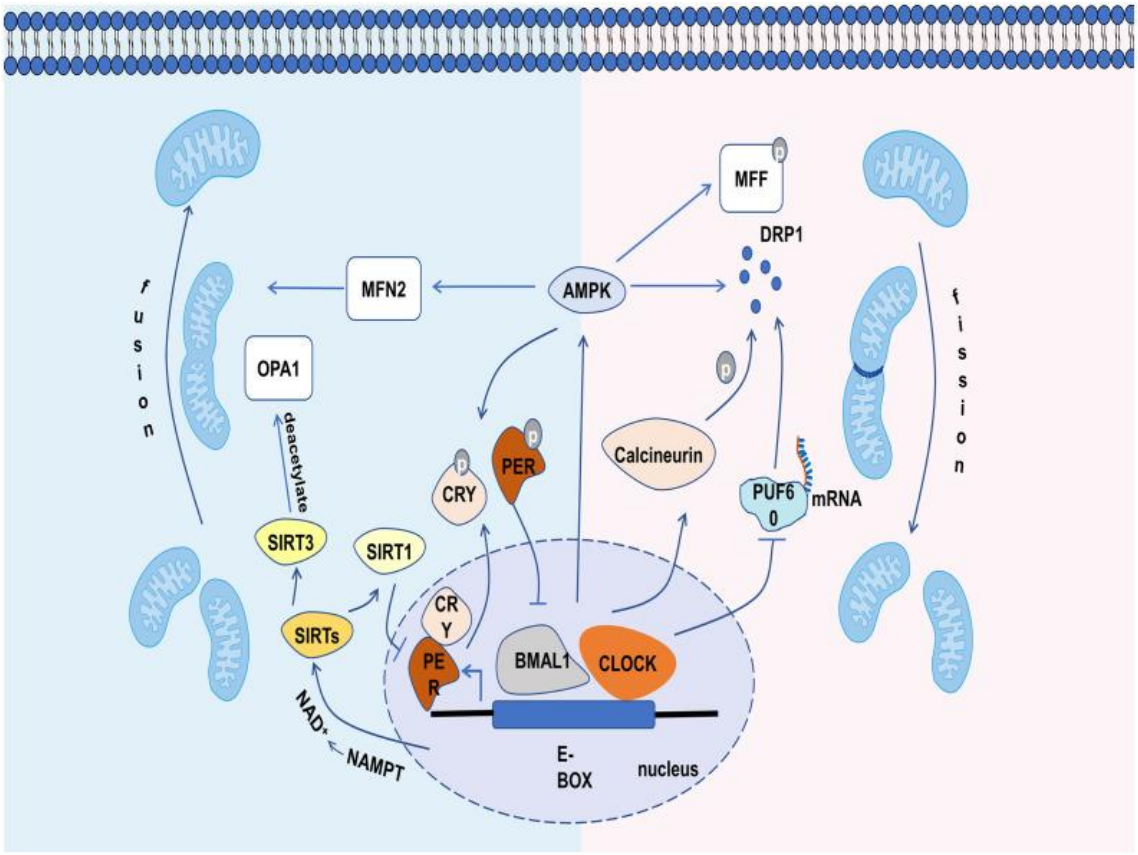

Figure 16. Circadian regulation of mitochondrial dynamics. The CLOCK:BMAL1 complex regulates sirtuins via NAD^+ biosynthesis, which in turn influence PER2 stability and OPA1 deacetylation. Calcineurin drives

the rhythmic dephosphorylation of DRP1, while CLOCK modulates DRP1 mRNA stability through PUF60. AMPK further connects energy status to circadian control by promoting fission, mitophagy, and MFN2-dependent fusion, as well as phosphorylating core clock components. Together, these mechanisms integrate circadian timing with mitochondrial fusion–fission balance. Obtained from (Jin et al., 2023).

After examining rhythmicity, we next evaluated the correlations between mitochondrial dynamics genes (**Figure 14**). Unlike the clock machinery, where correlations followed well-defined regulatory loops, the patterns here were fewer but still biologically coherent. The strongest association was a positive correlation between *Pgc1α* and *Mfn1*, which is consistent with the role of *Pgc1α* as a transcriptional regulator that promotes mitochondrial biogenesis and supports fusion-related pathways. A second significant positive correlation was observed between *Mfn1* and *Fis1*, which at first sight might appear contradictory, as MFN1 is involved in fusion whereas FIS1 contributes to fission (Chen et al., 2023). However, this could reflect the need for coordinated regulation between opposing processes to maintain mitochondrial network balance.

Other relationships, such as those involving *Mfn2* or *Drp1*, were weak and did not reach statistical significance, suggesting that their regulation may rely more heavily on post-transcriptional or post-translational mechanisms rather than co-regulated expression. This aligns with a recent review noting that mitochondrial dynamics, including the actions of MFN2 and DRP1, are largely regulated through post-transcriptional and post-translational mechanisms, for example via ER-dependent signaling pathways and phosphorylation events that control their localization and activity rather than their transcript levels (Bennett et al., 2022). Altogether, these results indicate that correlations among mitochondrial dynamics genes are fewer than in the circadian machinery, yet biologically plausible, reinforcing the need for interplay between fusion and fission components to sustain mitochondrial homeostasis.

Conclusion

In this study, we investigated the impact of grape seed (poly)phenol extract (GSPE) on hepatic circadian regulation, focusing on antioxidant responses, mitochondrial dynamics, and markers of oxidative stress under conditions of chronodisruption. Beyond the molecular analyses, it is important to note that chronodisruption also altered the feeding pattern of the animals, a change that was overtly manifested in the animals' feeding behavior, illustrating how environmental misalignment manifests at both behavioral and cellular levels.

Our results show that clock genes preserved rhythmicity under the 22-hour light–dark cycle, indicating a degree of adaptation. However, this rhythmicity was not identical to that of the canonical 24-hour cycle, as evidenced by altered expression profiles, particularly in transcriptional repressors such as *Cry1*. In parallel, disruption significantly modified the transcriptomic profile of several antioxidant and mitochondrial genes. Importantly, GSPE administration modulated these alterations in a time-dependent manner, with the most pronounced effects occurring during the active phase (ZT15–ZT21).

At the functional level, thiol levels revealed treatment-specific changes consistent with an antioxidant effect of GSPE, whereas GSH remained largely unaltered, suggesting that not all ROS-related pathways respond homogeneously to disruption or supplementation. Together, these findings highlight that the antioxidant response to chronodisruption is selective and that GSPE may exert its protective effects preferentially during phases of greater metabolic demand.

Despite the limited sample size per time point, which constrains the statistical robustness of some comparisons, the trends observed provide new insights into the temporal dimension of GSPE's action. Overall, our work supports the notion that chronodisruption alters hepatic homeostasis in a phase-specific manner and that dietary (poly)phenols such as GSPE can partially counteract these effects. Further studies will be necessary to validate these findings and to delineate more precisely how circadian misalignment reshapes redox balance and mitochondrial remodeling. Integrative approaches that consider both systemic and tissue-specific responses could provide deeper insights into the mechanisms linking chronodisruption, ROS generation, and mitochondrial dynamics.

References

Aragonès, G., Suárez, M., Ardid-Ruiz, A., Vinaixa, M., Rodríguez, M. A., Correig, X., Arola, L., & Bladé, C. (2016). Dietary proanthocyanidins boost hepatic NAD+ metabolism and SIRT1 expression and activity in a dose-dependent manner in healthy rats. *Scientific Reports, 6*(1), 24977. https://doi.org/10.1038/srep24977

Arreaza-Gil, V., Escobar-Martínez, I., Mulero, M., Muguerza, B., Suárez, M., Arola-Arnal, A., & Torres-Fuentes, C. (2023). Gut microbiota influences the photoperiod effects on proanthocyanidins bioavailability in diet-induced obese

rats. *Molecular Nutrition & Food Research, 67*(9), e2200600. https://doi.org/10.1002/mnfr.202200600

Arroyave-Ospina, J. C., Wu, Z., Geng, Y., & Moshage, H. (2021). Role of oxidative stress in the pathogenesis of non-alcoholic fatty liver disease: Implications for prevention and therapy. *Antioxidants, 10*(2), 174. https://doi.org/10.3390/antiox10020174

Ávila-Román, J., Soliz-Rueda, J. R., Bravo, F. I., Aragonès, G., Suárez, M., Arola-Arnal, A., Mulero, M., Salvadó, M.-J., Arola, L., Torres-Fuentes, C., & Muguerza, B. (2021). Phenolic compounds and biological rhythms: Who takes the lead? *Trends in Food Science & Technology, 113,* 77–85. https://doi.org/10.1016/j.tifs.2021.04.050

Ayyar, V. S., & Sukumaran, S. (2021). Circadian rhythms: Influence on physiology, pharmacology, and therapeutic interventions. *Journal of Pharmacokinetics and Pharmacodynamics, 48*(3), 321–338. https://doi.org/10.1007/s10928-021-09751-2

Bayo Jimenez, M. T., Frenis, K., Hahad, O., Steven, S., Cohen, G., Cuadrado, A., Münzel, T., & Daiber, A. (2022). Protective actions of nuclear factor erythroid 2-related factor 2 (NRF2) and downstream pathways against environmental stressors. *Free Radical Biology and Medicine, 187,* 72–91. https://doi.org/10.1016/j.freeradbiomed.2022.05.016

Bennett, C. F., Latorre-Muro, P., & Puigserver, P. (2022). Mechanisms of mitochondrial respiratory adaptation. *Nature Reviews Molecular Cell Biology, 23*(12), 817–835. https://doi.org/10.1038/s41580-022-00506-6

Boivin, D. B., Boudreau, P., & Kosmadopoulos, A. (2022). Disturbance of the circadian system in shift work and its health impact. *Journal of Biological Rhythms, 37*(1), 3–28. https://doi.org/10.1177/07487304211064218

Brillo, V., Chieregato, L., Leanza, L., Muccioli, S., & Costa, R. (2021). Mitochondrial dynamics, ROS, and cell signaling: A blended overview. *Life, 11*(4), 332. https://doi.org/10.3390/life11040332

Brüning, F., Noya, S. B., Bange, T., Koutsouli, S., Rudolph, J. D., Tyagarajan, S. K., Cox, J., Mann, M., Brown, S. A., & Robles, M. S. (2019). Sleep-wake cycles drive daily dynamics of synaptic phosphorylation. *Science, 366*(6462), eaav3617. https://doi.org/10.1126/science.aav3617

Chen, W., Zhao, H., & Li, Y. (2023). Mitochondrial dynamics in health and disease: Mechanisms and potential targets. *Signal Transduction and Targeted Therapy, 8*(1), 333. https://doi.org/10.1038/s41392-023-01547-9

Chhunchha, B., Kubo, E., & Singh, D. P. (2020). Clock protein Bmal1 and Nrf2 cooperatively control aging or oxidative response and redox homeostasis by regulating rhythmic expression of Prdx6. *Cells, 9*(8), 1861. https://doi.org/10.3390/cells9081861

Cortés-Espinar, A. J., Ibarz-Blanch, N., Soliz-Rueda, J. R., Bonafos, B., Feillet-Coudray, C., Casas, F., Bravo, F. I., Calvo, E., Ávila-Román, J., & Mulero, M. (2023). Rhythm and ROS: Hepatic chronotherapeutic features of grape seed proanthocyanidin extract treatment in cafeteria diet-fed rats. *Antioxidants, 12*(8), 1606. https://doi.org/10.3390/antiox12081606

Cortés-Espinar, A. J., Ibarz-Blanch, N., Soliz-Rueda, J. R., Calvo, E., Bravo, F. I., Mulero, M., & Ávila-Román, J. (2023). Abrupt photoperiod changes differentially modulate hepatic antioxidant response in healthy and obese rats: Effects of grape seed proanthocyanidin extract (GSPE). *International Journal of Molecular Sciences, 24*(23), 17057. https://doi.org/10.3390/ijms242317057

Cui, Y., Yin, Y., Li, S., Xie, Y., Wu, Z., Yang, H., Qian, Q., & Li, X. (2022). Apple polyphenol extract targets circadian rhythms to improve liver biological clock and lipid homeostasis in C57BL/6 male mice with mistimed high-fat diet feeding. *Journal of Functional Foods, 92,* 105051. https://doi.org/10.1016/j.jff.2022.105051

Fagiani, F., Di Marino, D., Romagnoli, A., Travelli, C., Voltan, D., Di Cesare Mannelli, L., Racchi, M., Govoni, S., & Lanni, C. (2022). Molecular regulations of circadian rhythm and implications for physiology and diseases. *Signal Transduction and Targeted Therapy, 7*(1), 41. https://doi.org/10.1038/s41392-022-00899-y

Fishbein, A. B., Knutson, K. L., & Zee, P. C. (2021). Circadian disruption and human health. *Journal of Clinical Investigation, 131*(19), e148286. https://doi.org/10.1172/JCI148286

Gabriel, B. M., Altıntaş, A., Smith, J. A. B., Sardon-Puig, L., Zhang, X., Basse, A. L., Laker, R. C., Gao, H., Liu, Z., Dollet, L., Treebak, J. T., Zorzano, A., Huo, Z., Rydén, M., Lanner, J. T., Esser, K. A., Barrès, R., Pillon, N. J., Krook, A., & Zierath, J. R. (2021). Disrupted circadian oscillations in type 2 diabetes are linked to

altered rhythmic mitochondrial metabolism in skeletal muscle. *Science Advances, 7*(43), eabi9654. https://doi.org/10.1126/sciadv.abi9654

Gao, S., & Hu, J. (2021). Mitochondrial fusion: The machineries in and out. *Trends in Cell Biology, 31*(1), 62–74. https://doi.org/10.1016/j.tcb.2020.09.008

Gao, W., Guo, L., Yang, Y., Wang, Y., Xia, S., Gong, H., Zhang, B.-K., & Yan, M. (2022). Dissecting the crosstalk between Nrf2 and NF-κB response pathways in drug-induced toxicity. *Frontiers in Cell and Developmental Biology, 9,* 809952. https://doi.org/10.3389/fcell.2021.809952

Greco, C. M., Koronowski, K. B., Smith, J. G., Shi, J., Kunderfranco, P., Carriero, R., Chen, S., Samad, M., Welz, P.-S., Zinna, V. M., Mortimer, T., Chun, S. K., Shimaji, K., Sato, T., Petrus, P., Kumar, A., Vaca-Dempere, M., Deryagin, O., Van, C., … Sassone-Corsi, P. (2021). Integration of feeding behavior by the liver circadian clock reveals network dependency of metabolic rhythms. *Science Advances, 7*(39), eabi7828. https://doi.org/10.1126/sciadv.abi7828

Griffith, O. W. (1980). Determination of glutathione and glutathione disulfide using glutathione reductase and 2-vinylpyridine. *Analytical Biochemistry, 106*(1), 207–212. https://doi.org/10.1016/0003-2697(80)90139-6

Guan, D., & Lazar, M. A. (2021). Interconnections between circadian clocks and metabolism. *Journal of Clinical Investigation, 131*(15), e148278. https://doi.org/10.1172/JCI148278

Huang, C. C.-Y., Ko, M. L., Vernikovskaya, D. I., & Ko, G. Y.-P. (2012). Calcineurin serves in the circadian output pathway to regulate the daily rhythm of L-type voltage-gated calcium channels in the retina. *Journal of Cellular Biochemistry, 113*(3), 911–922. https://doi.org/10.1002/jcb.23419

Ince, L. M. (2022). Introduction to biological rhythms: A brief history of chronobiology and its relevance to parasite immunology. *Parasite Immunology, 44*(3), e12905. https://doi.org/10.1111/pim.12905

Jin, Z., Ji, Y., Su, W., Zhou, L., Wu, X., Gao, L., Guo, J., Liu, Y., Zhang, Y., Wen, X., Xia, Z.-Y., Xia, Z., & Lei, S. (2023). The role of circadian clock-controlled mitochondrial dynamics in diabetic cardiomyopathy. *Frontiers in Immunology, 14,* 1142512. https://doi.org/10.3389/fimmu.2023.1142512

Jocelyn P. C. (1987). Spectrophotometric assay of thiols. *Methods in enzymology*, *143*, 44–67. https://doi.org/10.1016/0076-6879(87)43013-9

Jomova, K., Raptova, R., Alomar, S. Y., Alwasel, S. H., Nepovimova, E., Kuca, K., & Valko, M. (2023). Reactive oxygen species, toxicity, oxidative stress, and antioxidants: Chronic diseases and aging. *Archives of Toxicology, 97*(10), 2499–2574. https://doi.org/10.1007/s00204-023-03562-9

Juan, C. A., Pérez de la Lastra, J. M., Plou, F. J., & Pérez-Lebeña, E. (2021). The chemistry of reactive oxygen species (ROS) revisited: Outlining their role in biological macromolecules (DNA, lipids and proteins) and induced pathologies. *International Journal of Molecular Sciences, 22*(9), 4642. https://doi.org/10.3390/ijms22094642

Lai, Y., Li, M., Liao, X., & Zou, L. (2021). Smartphone-assisted colorimetric detection of glutathione and glutathione reductase activity in human serum and mouse liver using hemin/G-quadruplex DNAzyme. *Molecules, 26*(16), 5016. https://doi.org/10.3390/molecules26165016

Lang, Y., Gao, N., Zang, Z., Meng, X., Lin, Y., Yang, S., Yang, Y., Jin, Z., & Li, B. (2024). Classification and antioxidant assays of polyphenols: A review. *Journal of Future Foods, 4*(3), 193–204. https://doi.org/10.1016/j.jfutfo.2023.07.002

Laothamatas, I., Rasmussen, E. S., Green, C. B., & Takahashi, J. S. (2023). Metabolic and chemical architecture of the mammalian circadian clock. *Cell Chemical Biology, 30*(9), 1033–1052. https://doi.org/10.1016/j.chembiol.2023.08.014

Lee, Y. (2021). Roles of circadian clocks in cancer pathogenesis and treatment. *Experimental & Molecular Medicine, 53*(10), 1529–1538. https://doi.org/10.1038/s12276-021-00681-0

Lee, Y., Field, J. M., & Sehgal, A. (2021). Circadian rhythms, disease and chronotherapy. *Journal of Biological Rhythms, 36*(6), 503–531. https://doi.org/10.1177/07487304211044301

Lim, J. C., Suzuki-Kerr, H., Nguyen, T. X., Lim, C. J. J., & Poulsen, R. C. (2022). Redox homeostasis in ocular tissues: Circadian regulation of glutathione in the lens? *Antioxidants, 11*(8), 1516. https://doi.org/10.3390/antiox11081516

Livak, K. J., & Schmittgen, T. D. (2001). Analysis of relative gene expression data using real-time quantitative PCR and the 2−ΔΔCT method. *Methods, 25*(4), 402–408. https://doi.org/10.1006/meth.2001.1262

Marino, A., Battaglini, M., Moles, N., & Ciofani, G. (2022). Natural antioxidant compounds as potential pharmaceutical tools against neurodegenerative

diseases. *ACS Omega,* *7*(30), 25974–25990. https://doi.org/10.1021/acsomega.2c03291

McClean, C., & Davison, G. W. (2022). Circadian clocks, redox homeostasis, and exercise: Time to connect the dots? *Antioxidants, 11*(2), 256. https://doi.org/10.3390/antiox11020256

Meléndez-Fernández, O. H., Liu, J. A., & Nelson, R. J. (2023). Circadian rhythms disrupted by light at night and mistimed food intake alter hormonal rhythms and metabolism. *International Journal of Molecular Sciences, 24*(4), 3392. https://doi.org/10.3390/ijms24043392

Mezhnina, V., Ebeigbe, O. P., Poe, A., & Kondratov, R. V. (2022). Circadian control of mitochondria in reactive oxygen species homeostasis. *Antioxidants & Redox Signaling, 37*(10–12), 647–663. https://doi.org/10.1089/ars.2021.0274

Moselhy, M., Abd-Elhafez, K., El-Kholany, E., Gohar, M., & Nasr, N. (2023). Antimicrobial, antioxidant and anticancer properties of globe artichoke and grape by-products as a source of bioactive phenolic compounds. *Egyptian Journal of Chemistry.* Advance online publication. https://doi.org/10.21608/ejchem.2022.173125.7166

Moškon, M. (2020). CosinorPy: A Python package for cosinor-based rhythmometry. *BMC Bioinformatics, 21*(1), 485. https://doi.org/10.1186/s12859-020-03830-w

Narasimamurthy, R., & Virshup, D. M. (2017). Molecular mechanisms regulating temperature compensation of the circadian clock. *Frontiers in Neurology, 8,* 161. https://doi.org/10.3389/fneur.2017.00161

Pereira, D. G., Afonso, A., & Medeiros, F. M. (2015). Overview of Friedman's test and post-hoc analysis. *Communications in Statistics - Simulation and Computation,* *44*(10), 2636–2653. https://doi.org/10.1080/03610918.2014.931971

Pickel, L., & Sung, H.-K. (2020). Feeding rhythms and the circadian regulation of metabolism. *Frontiers in Nutrition, 7,* 39. https://doi.org/10.3389/fnut.2020.00039

Pugliane, K. C., Castelo-Branco, R., Araújo, K. K. B. C., Pereira, J. C., Leal, J. C. de O., Koike, B. D. V., Fontenele-Araujo, J., da Silva, C. A., & Barbosa, F. F. (2025). Dissociation of circadian rhythms in adolescent rats affects object recognition and spatial recognition memories. *Physiology & Behavior, 292,* 114824. https://doi.org/10.1016/j.physbeh.2025.114824

Rajha, H. N., Paule, A., Aragonès, G., Barbosa, M., Caddeo, C., Debs, E., Dinkova, R., Eckert, G. P., Fontana, A., Gebrayel, P., Maroun, R. G., Napolitano, A., Panzella, L., Pasinetti, G. M., Stevens, J. F., Schieber, A., & Edeas, M. (2022). Recent advances in research on polyphenols: Effects on microbiota, metabolism, and health. *Molecular Nutrition & Food Research, 66*(1), e2100670. https://doi.org/10.1002/mnfr.202100670

Reagan-Shaw, S., Nihal, M., & Ahmad, N. (2008). Dose translation from animal to human studies revisited. *The FASEB Journal, 22*(3), 659–661. https://doi.org/10.1096/fj.07-9574LSF

Rodríguez, R. M., Cortés-Espinar, A. J., Soliz-Rueda, J. R., Feillet-Coudray, C., Casas, F., Colom-Pellicer, M., Aragonès, G., Ávila-Román, J., Muguerza, B., Mulero, M., & Salvadó, M. J. (2022). Time-of-day circadian modulation of grape-seed procyanidin extract (GSPE) in hepatic mitochondrial dynamics in cafeteria-diet-induced obese rats. *Nutrients, 14*(4), 774. https://doi.org/10.3390/nu14040774

Rodriguez-Mateos, A., Le Sayec, M., & Cheok, A. (2024). Dietary (poly)phenols and cardiometabolic health: From antioxidants to modulators of the gut microbiota. *Proceedings of the Nutrition Society, 83*(1), 1–11. https://doi.org/10.1017/S0029665124000156

Romero-Durán, M. A., Silva-García, O., Perez-Aguilar, J. M., & Baizabal-Aguirre, V. M. (2024). Mechanisms of Keap1/Nrf2 modulation in bacterial infections: Implications in persistence and clearance. *Frontiers in Immunology, 15,* 1508787. https://doi.org/10.3389/fimmu.2024.1508787

Schober, P., Boer, C., & Schwarte, L. A. (2018). Correlation coefficients: Appropriate use and interpretation. *Anesthesia & Analgesia, 126*(5), 1763–1768. https://doi.org/10.1213/ANE.0000000000002864

Schwartz, M. D., Cambras, T., Díez-Noguera, A., Campuzano, A., Oda, G. A., Yamazaki, S., & de la Iglesia, H. O. (2022). Coupling between subregional oscillators within the suprachiasmatic nucleus determines free-running period in the rat. *Journal of Biological Rhythms, 37*(6), 620–630. https://doi.org/10.1177/07487304221126074

Sharma, A., Shahzad, B., Rehman, A., Bhardwaj, R., Landi, M., & Zheng, B. (2019). Response of phenylpropanoid pathway and the role of polyphenols in

plants under abiotic stress. *Molecules, 24*(13), 2452. https://doi.org/10.3390/molecules24132452

Sies, H. (2021). Oxidative eustress: On constant alert for redox homeostasis. *Redox Biology, 41,* 101867. https://doi.org/10.1016/j.redox.2021.101867

Soni, S. K., Basu, P., Singaravel, M., Sharma, R., Pandi-Perumal, S. R., Cardinali, D. P., & Reiter, R. J. (2021). Sirtuins and the circadian clock interplay in cardioprotection: Focus on sirtuin 1. *Cellular and Molecular Life Sciences, 78*(6), 2503–2515. https://doi.org/10.1007/s00018-020-03713-6

Spaleniak, W., & Cuendet, M. (2023). Resveratrol as a circadian clock modulator: Mechanisms of action and therapeutic applications. *Molecular Biology Reports, 50*(7), 6159–6170. https://doi.org/10.1007/s11033-023-08513-2

Sun, Q., Zeng, C., Du, L., & Dong, C. (2021). Mechanism of circadian regulation of the NRF2/ARE pathway in renal ischemia reperfusion. *Experimental and Therapeutic Medicine, 21*(3), 190. https://doi.org/10.3892/etm.2021.9622

Van Drunen, R., & Eckel-Mahan, K. (2021). Circadian rhythms of the hypothalamus: From function to physiology. *Clocks & Sleep, 3*(1), 189–226. https://doi.org/10.3390/clockssleep3010012

Wang, R., Liang, L., Matsumoto, M., Iwata, K., Umemura, A., & He, F. (2023). Reactive oxygen species and NRF2 signaling, friends or foes in cancer? *Biomolecules, 13*(2), 353. https://doi.org/10.3390/biom13020353

Wende, A. R., Young, M. E., Chatham, J., Zhang, J., Rajasekaran, N. S., & Darley-Usmar, V. M. (2016). Redox biology and the interface between bioenergetics, autophagy and circadian control of metabolism. *Free Radical Biology and Medicine, 100,* 94–107. https://doi.org/10.1016/j.freeradbiomed.2016.05.022

Wobbrock, J. O., Findlater, L., Gergle, D., & Higgins, J. J. (2011). The aligned rank transform for nonparametric factorial analyses using only ANOVA procedures. *Proceedings of the SIGCHI Conference on Human Factors in Computing Systems,* 143–146. https://doi.org/10.1145/1978942.1978963

Xu, L., Lin, J., Liu, Y., Hua, B., Cheng, Q., Lin, C., Yan, Z., Wang, Y., Sun, N., Qian, R., & Lu, C. (2022). CLOCK regulates Drp1 mRNA stability and mitochondrial homeostasis by interacting with PUF60. *Cell Reports, 39*(2), 110635. https://doi.org/10.1016/j.celrep.2022.110635

Yapa, N. M. B., Lisnyak, V., Reljic, B., & Ryan, M. T. (2021). Mitochondrial dynamics in health and disease. *FEBS Letters, 595*(8), 1184–1204. https://doi.org/10.1002/1873-3468.14077

Zaidi, S. K., Shen, W.-J., Cortez, Y., Bittner, S., Bittner, A., Arshad, S., Huang, T.-T., Kraemer, F. B., & Azhar, S. (2021). SOD2 deficiency-induced oxidative stress attenuates steroidogenesis in mouse ovarian granulosa cells. *Molecular and Cellular Endocrinology, 519,* 110888. https://doi.org/10.1016/j.mce.2020.110888

Zeng, Y., Guo, Z., Wu, M., Chen, F., & Chen, L. (2024). Circadian rhythm regulates the function of immune cells and participates in the development of tumors. *Cell Death Discovery, 10*(1), 199. https://doi.org/10.1038/s41420-024-01960-1

Zerihun, M., Sukumaran, S., & Qvit, N. (2023). The Drp1-mediated mitochondrial fission protein interactome as an emerging core player in mitochondrial dynamics and cardiovascular disease therapy. *International Journal of Molecular Sciences, 24*(6), 5785. https://doi.org/10.3390/ijms24065785

Zhang, W., Xiong, Y., Tao, R., Panayi, A. C., Mi, B., & Liu, G. (2022). Emerging insight into the role of circadian clock gene BMAL1 in cellular senescence. *Frontiers in Endocrinology, 13,* 915139. https://doi.org/10.3389/fendo.2022.915139

Zhang, Z., Zeng, P., Gao, W., Zhou, Q., Feng, T., & Tian, X. (2021). Circadian clock: A regulator of the immunity in cancer. *Cell Communication and Signaling, 19*(1), 37. https://doi.org/10.1186/s12964-021-00721-2

Self evaluation

When I began this Final Degree Project, my main goal was to learn how to manage a scientific project and to strengthen my ability to interpret complex biological results. I knew the topic, chronodisruption, oxidative stress, and mitochondrial dynamics, would demand effort, but I was motivated by the chance to contribute, even modestly, to understanding how polyphenols may modulate the organism's response. Throughout the process I reinforced technical skills (gene expression analysis, data handling, rhythmicity and correlation approaches) and learned to defend methodological decisions. I also improved my scientific writing, moving toward an academic style, and gained deeper insight into statistics, since the complex design required alternatives beyond standard ANOVA. At the same time, I recognized that time and stress management are areas where I need to improve, as pressure and perfectionism often reduce fluency. On a personal level, this project confirmed my vocation for biomedical and clinical research. I especially value connecting different layers, from physiology to molecular regulation, and working in contexts that require curiosity and perseverance. Despite the difficulties, I am satisfied with the path taken, aware that its value lies not only in the outcome but also in the learning process and the maturity gained.

Appendix

Supplementary Table 1. Correlation analysis between core clock genes

Variable-X	Variable-Y	p_value	rho	FDR
Nampt	*Cry1*	0.181	0.169	0.585
Nampt	*Per2*	0.000	0.695	0.000
Nampt	*Bmal1*	0.000	-0.626	0.000
Nampt	*Sirt1*	0.123	0.195	0.467
Nampt	*Rora*	0.737	-0.043	0.908
Nampt	*Clock*	0.000	-0.496	0.001
Nampt	*Rev-erb-a*	0.106	0.204	0.450
Cry1	*Per2*	0.000	0.456	0.005
Cry1	*Bmal1*	0.104	0.205	0.450
Cry1	*Sirt1*	0.012	-0.313	0.161
Cry1	*Rora*	0.028	0.274	0.240
Cry1	*Clock*	0.891	-0.018	0.962
Cry1	*Rev-erb-a*	0.000	-0.532	0.000
Per2	*Bmal1*	0.000	-0.618	0.000
Per2	*Sirt1*	0.495	0.087	0.795
Per2	*Rora*	0.510	0.084	0.795
Per2	*Clock*	0.000	-0.566	0.000
Per2	*Rev-erb-a*	0.433	0.100	0.750
Bmal1	*Sirt1*	0.001	-0.404	0.023
Bmal1	*Rora*	0.416	0.103	0.740
Bmal1	*Clock*	0.000	0.795	0.000
Bmal1	*Rev-erb-a*	0.000	-0.598	0.000
Sirt1	*Rora*	0.948	0.008	0.977
Sirt1	*Clock*	0.144	-0.185	0.520
Sirt1	*Rev-erb-a*	0.023	0.283	0.232
Rora	*Clock*	0.264	0.142	0.654
Rora	*Rev-erb-a*	0.074	-0.225	0.382
Clock	*Rev-erb-a*	0.002	-0.379	0.040

Pairwise associations were evaluated between Cry1, Per2, Bmal1, Clock, Rev-erb-α, Rorα. The table reports Spearman's correlation coefficients (rho), corresponding p-values, and FDR-adjusted significance levels.

Supplementary Table 2. Correlation values for oxidative stress–related genes

Variable-X	Variable-Y	p_value	rho	FDR
Sod1	*Sod2*	0.0175	0.2961	0.203
Sod1	*Catalase*	0.0669	0.2305	0.370
Sod1	*Gpx1*	0.0177	0.2956	0.203
Sod1	*Gsr*	0.9379	-0.0099	0.977
Sod1	*Nrf2*	0.0001	0.4824	0.002
Sod1	*Keap1*	0.0001	0.4625	0.004
Sod2	*Catalase*	0.0095	0.3220	0.152
Sod2	*Gpx1*	0.9230	0.0123	0.973
Sod2	*Gsr*	0.4055	0.1058	0.740
Sod2	*Nrf2*	0.0242	0.2816	0.232
Sod2	*Keap1*	0.6002	0.0668	0.842
Catalase	*Gpx1*	0.0825	0.2187	0.404
Catalase	*Gsr*	0.0751	0.2240	0.382
Catalase	*Nrf2*	0.0199	0.2905	0.219
Catalase	*Keap1*	0.2038	0.1610	0.609
Gpx1	*Gsr*	0.1869	-0.1671	0.585
Gpx1	*Nrf2*	0.0002	0.4493	0.006
Gpx1	*Keap1*	0.4286	0.1007	0.748
Gsr	*Nrf2*	0.2866	-0.1353	0.669
Gsr	*Keap1*	0.9176	0.0132	0.973
Nrf2	*Keap1*	0.0012	0.3950	0.029

Pairwise Spearman's coefficients (rho), associated p-values and FDR-adjusted significance levels are presented for Sod1. Sod2. Catalase. Gpx1. Gsr. Nrf2. and Keap1.

Supplementary Table 3. Correlation analysis among mitochondrial dynamics–related genes.

Variable-X	Variable-Y	*P* value	rho	FDR
Mfn1	*Mfn2*	0.124	0.194	0.467
Mfn1	*Fis1*	0.378	0.112	0.740
Mfn1	*Drp1*	0.230	0.152	0.628
Mfn1	*Pgc1a*	0.368	0.114	0.740
Mfn2	*Fis1*	0.015	0.303	0.183
Mfn2	*Drp1*	0.667	0.055	0.872
Mfn2	*Pgc1a*	0.002	0.379	0.040
Fis1	*Drp1*	0.417	0.103	0.740
Fis1	*Pgc1a*	0.055	0.241	0.351
Drp1	*Pgc1a*	0.479	0.090	0.784
Mfn1	*Mfn2*	0.124	0.194	0.467

Pairwise associations were evaluated between Mfn1, Mfn2, Fis1, Drp1, and Pgc1α. The table reports Spearman's correlation coefficients (rho), corresponding p-values, and FDR-adjusted significance levels.